crystals

MDPI

Review

Conductive Covalent Organic Frameworks Meet Micro-Electrical Energy Storage: Mechanism, Synthesis and Applications—A Review

Chengfei Qian [1,†], Ronghao Wang [1,†], Feng Yu [1,2], He Liu [1,2], Cong Guo [1,2], Kaiwen Sun [3], Jingfa Li [1,2] and Weizhai Bao [1,2,*]

[1] Institute of Advanced Materials and Flexible Electronics (IAMFE), School of Chemistry and Materials Science, Nanjing University of Information Science and Technology, Nanjing 210044, China
[2] Department of Materials Physics, School of Chemistry and Materials Science, Nanjing University of Information Science and Technology, Nanjing 210044, China
[3] Australian Centre for Advanced Photovoltaics, School of Photovoltaic and Renewable Energy Engineering, University of New South Wales, Sydney, NSW 2052, Australia
* Correspondence: weizhai.bao@nuist.edu.cn
† These authors contributed equally to this work.

Abstract: Conductive covalent organic frameworks (c-COFs) have been widely used in electrochemical energy storage because of their highly adjustable porosity and modifiable skeletons. Additionally, the fast carrier migration and ion catalysis requirements of micro-electrochemical energy storages (MEESs) are perfectly matched with c-COFs. Therefore, c-COFs show great potential and unlimited prospects in MEESs. However, the main organic component blocks electron conduction, and the internal active sites are difficult to fully utilize, which limits the application of c-COFs. In order to overcome these obstacles, a great deal of research has been conducted on conductivity enhancement. This review first focuses on the exploration of c-COFs in the field of electrical conductivity. Then, the mechanism and explanation of the effect of synthesis on electrical conductivity enhancement are discussed, which emphasizes the range and suitability of c-COFs in MEESs. Finally, the excellent performance characteristics of c-COFs are demonstrated from the MEES perspective, with key points and potential challenges addressed. This review also predicts the direction of development of c-COFs in the future.

Keywords: covalent organic frameworks; micro-electrochemical energy storage; density functional theory; conductive

Citation: Qian, C.; Wang, R.; Yu, F.; Liu, H.; Guo, C.; Sun, K.; Li, J.; Bao, W. Conductive Covalent Organic Frameworks Meet Micro-Electrical Energy Storage: Mechanism, Synthesis and Applications—A Review. *Crystals* **2022**, *12*, 1405. https://doi.org/10.3390/cryst12101405

Academic Editor: Suresh Kannan Balasingam

Received: 2 September 2022
Accepted: 30 September 2022
Published: 4 October 2022

1. Introduction

With the rapid development of the internet and information technology, human society is also accelerating into a new era of digitalization and intelligence. With the help of advanced micro-electronic devices, accurately treating diseases, obtaining environmental information, and monitoring equipment performance have become more accessible [1–9]. In the face of the diverse requirements of various applications, the design of micro-electronic devices needs to be considered in dimension, shape, performance, flexibility, and other aspects [10–12]. At the same time, as an important part of micro-electronic devices, micro-electrochemical energy storage (MEES) system has become the focus to meet the development requirements of micro-electronic devices. MEES devices include micro-batteries and micro-supercapacitors. At first, this refers to miniaturized batteries or capacitors whose sizes are smaller than those of traditional electrochemical energy storage devices in at least one dimension. Later, this extended to miniaturized energy storage devices with non-traditional structures or special capabilities. This has very broad application prospects in various situations, especially in unusual environments, such as micro-robots, wearable devices, and medical implants [13–15].

Similar to conventional electrochemical energy storage devices, the overall optimization of MEES electrode materials and devices is the focus of its development. At present, the overall optimization of the device has been fully studied in most research, but the electrode material suitable for MEES is still unknown [16–18]. Compared with traditional electrochemical energy storage devices, flexible, designable, and customizable electrode materials are required to seamlessly integrate with various environments [19,20]. Unfortunately, most of the traditional electrochemical energy storage electrodes are fixed in shape, poor in flexibility, and large in volume, which means they cannot meet the strict requirements of the new generation of micro-electronic products [21–23]. Therefore, extensive research is being conducted with the goal of improving the energy storage capacity of MEES without sacrificing the power density and cycling stability of the electrode material.

Under such strict requirements, covalent organic framework (COF) materials come into view [24–26]. This organic framework connected by covalent bonds provides an excellent material for this pioneering MEES development (Figure 1). Its high porosity, aligned ion channel, and dynamic reversible crystal structure can meet MEES requirements for stretchability, bendability, and designability, while the energy density and power density are not far behind the current commercial electrode materials [27,28]. COFs have many advantages required for MEES devices, but as a branch of organic compounds, their low conductivity becomes their limitation in energy storage materials [29]. Generally, sufficient conductive agent is added to improve the conductivity of the slurry when preparing the electrode, which will greatly reduce the specific mass capacity of the MEES electrode. Reducing the amount of conductive and binder can improve the electrochemical performance of MEES. Therefore, many studies have been carried out to optimize the conductivity of COFs. In 2019, a COF that generates uninterrupted *p*-electron delocalization in the two-dimensional (2D) direction was reported by introducing a plane-conjugated triazine nucleus into a 2D framework. Its large specific surface area and unique nano-fiber structure make it a good application in micro-flexible supercapacitors [30]. In addition, due to the interaction of 3,5-dicyano-2,4,6-trimethylpyridine, and 1,3,5-triazine, the C=C bond in the synthesized COF is not replaced, which is conducive to improving the *p*-type electron delocalization of the 2D sp2 carbon chain [31,32]. It is a good method to enhance the conductivity of COF.

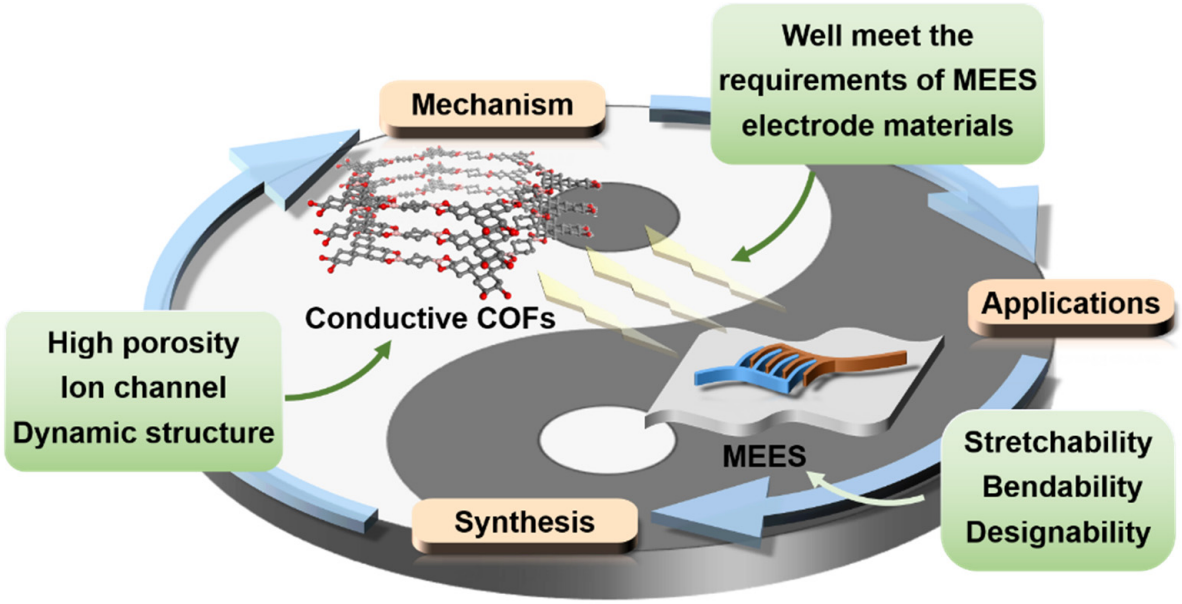

Figure 1. Illustration of the customization of electrode materials for MEES devices via various strategies.

Herein, we first focus on the exploration of conductive COFs (c-COFs) in the field of electrical conductivity. Then, the mechanism and explanation of the effect of synthesis

on electrical conductivity enhancement are discussed, which emphasizes the range and suitability of c-COFs in MEESs. Finally, the excellent performance characteristics of c-COFs are demonstrated from the MEES perspective, with key points and potential challenges addressed. This review also predicts the direction of development of c-COFs in the future.

2. Conductivity Enhancement Mechanism

2.1. Strategies on Conductivity Enhancing

COF is a porous polymer crystal that allows organic ligand units to combine precisely at the atomic scale, repeatedly creating ordered skeletal structures and pore channels [33–35]. Due to this, researchers can fine-tune COFs to find breakthroughs that reduce the difficulty of electron migration. In this section, we summarize the strategies for conductivity modification of COFs experimentally and theoretically, and discuss the relationship between methods and conductivity, the mechanisms of electronic conductivity changes, and design strategies.

2.1.1. Ligand-Bond Coordination Strategies

To construct c-COFs, much effort has been focused on introducing conductive ligands, such as 4-thiophenephenyl, imidazolate and other ligand units into the framework skeleton. Among them, redox-active groups, such as quinones, semiquinones, and catecholates, can be incorporated into COFs to enhance conductivity [36,37].

It is a nice strategy to construct c-COFs by promoting proper spatial and energy overlap of organic ligand orbitals through covalent bonds to achieve charge transfer [38]. Coordination bonds in c-COFs composed of specific organic ligands have matching energy levels and good orbital overlap, which can generate long-distance charge transfer pathways, which is beneficial for improving charge transfer.

In addition, a continuous conjugated structure is introduced on the main chain, and the electron in the conjugated system is delocalized at the level of the whole molecular main chain to conduct electricity. In conductive coordination polymers, organic ligands can be used as carrier fluids, while redox-active ligands can be delocalized by continuous conjugation. Therefore, the conductivity of COFs can be achieved by linking redox-active ligands. 2D planar redox ligands, such as 2,3,6,7,10,11-hexahydroxytriphenylene (HHTP), 2,3,6,7,10,11-hexaaminotriphenylene (HITP), 1,2,3,4,5,6-Benzenehexamine (HAB), and 2,3,6,7,10,11-Triphenylenehexathiol (HTTP), usually show good conductivity due to the effective overlap and continuous conjugation of the front orbitals of organic ligands, which is due to the electron delocalization in the plane.

2.1.2. Ligand A—A Stacking Strategy

Organic segments in COFs with non-covalent interactions can form a space-charge transport pathway. For organic molecules, effective charge transfer requires that a charge can be transferred from one molecule to another without being captured or dispersed [39,40]. In a similar manner, organic ligands with a tendency to form A-A stack structures can give COFs excellent electrical conductivity. A typical example of this is based on the research of the c-COFs of hexadecafluorophthalocyanines and octaminophthalocyanines [41]. Periodic and ordered phthalocyanine columns with A-A stacking have good permanent porosity and chemical stability. The conductivity reaches 12.7 S m^{-1} or more. The A-A stack structure can form strong π-π interaction between layers due to the superposition of faces [42]. This A-A stacked structure can form an interaction between layers due to the superposition of each side. The interaction of atoms in the conjugated system results in the change of π (or p) electron distribution in the system. This weak interaction, also known as π-π interaction, facilitates charge transfer [43]. In addition, it is found that the neatly arranged 2D COFs and the intrinsic free radicals are also conducive to electron diffusion, which brings high conductivity to COFs.

2.1.3. Proton Grotthuss Transfer Strategy

In the hopping transport mechanism, electrically loaded fluids (electrons or holes) are positioned at specific positions with discrete energy levels and jump between adjacent positions. Jump transport depends on charge jumps between adjacent units in a given situation (the spatial distance is narrow and the energy difference between adjacent units regulated by redox activity is small). In addition, skip transport is closely related to temperature, and higher temperatures lead to higher conductivity. This jumping mechanism enables protons to jump by means of hydrogen bonding and molecular rearrangement, which is called the Grotthuss mechanism [44–46].

For the MEES equipment, fast charge and discharge and high energy density are its pursuits. Proton Grotthuss transfer can promote the redox reaction of the electrode, which can make the MEES equipment have better performance, especially if the micro-supercapacitor has outstanding performance. A novel COF was synthesized by combining tris(4-formylphenyl)amine (TFPA) ligand with Azo-NHBoc molecule (Figure 2b–d) [47]. The capacitance of COF was up to 440 F g^{-1} (Figure 2e), higher than that of traditional capacitor materials.

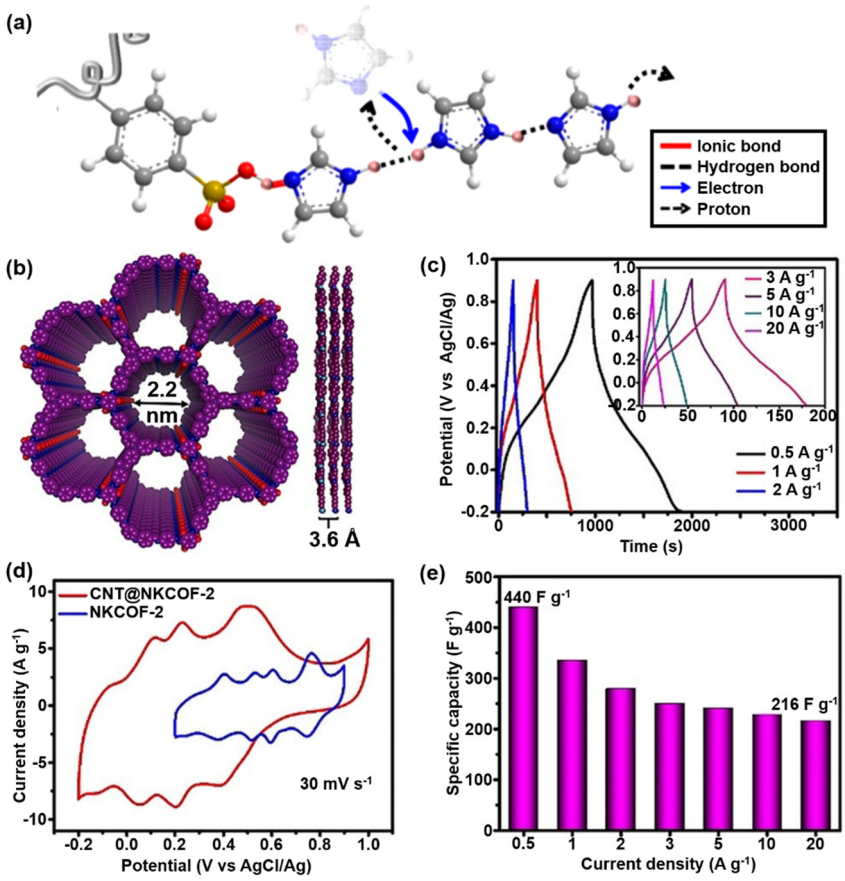

Figure 2. Grotthuss transfer strategy has positive effects on electrochemical performance. (**a**) Schematic illustrations of the Grotthuss transport mechanisms [44]. Copyright 2014, American Chemical Society. (**b**) Simulated structure of NKCOF–8. (**c**) Galvanostatic charge-discharge curves of CNT/NKCOF–2 at different current densities. (**d**) CV curves of NKCOF–2 and CNT/NKCOF–2 at a scan rate of 30 mV s^{-1}. (**e**) Specific capacities of CNT/NKCOF–2 at different current densities [47]. Copyright 2021, Wiley-VCH.

In addition, in order to prove the promoting effect of the Grotthuss mechanism on electrode materials, scholars studied and analyzed the proton conductivity and theoretical proton transfer activation energy of this new COF [48]. It is confirmed that the proton Grotthuss transfer mechanism can rapidly transfer protons to the redox site buried deep in

the stacked frame, which can promote the reaction kinetics, accelerate the reaction process, and improve the utilization rate of the active site.

2.1.4. Post-Synthetic Modification Strategy

It is challenging to synthesize COFs with high electrical conductivity for the first step. Post-synthetic modification has become an important strategy for enhancing the conductivity of COFs [49,50]. After the synthesis of COF, chemical modification is carried out without destroying the precursor of the COF's original structure, and new functional groups or specific point modifications are introduced to improve the electrical conductivity. Meanwhile, in post-synthetic modification, functional groups are introduced or attached to the pore surface of COFs while maintaining structural integrity [51].

Polymer Introduction

Weikai Wang and co-workers found that COF-316 has the advantages of rich porosity, inter-connected hollow regions, and easy modification, and can be effectively combined with conductive polypyrrole materials to produce more excellent electrochemical characteristics (Figure 3a) [52]. The hydrogen bond interaction in a uniform composite structure improves the charge transfer efficiency and enhances the stability of the structure (Figure 3b). In the study of COFs used in energy storage systems, Mulzer et al. introduced PEDOT into the post-synthetic modification of COF films to enhance the electrical conductivity and significantly improve electrochemical reactions [53]. The improved material has tens of times the current response and high-cycle stability in supercapacitors (Figure 3c,d). In addition, for 2D porphyrin-based or phthalocyanine-based COFs, post-processing can significantly improve the ease of ion migration, thus, flexibly improving the sensing performance of the COF [54].

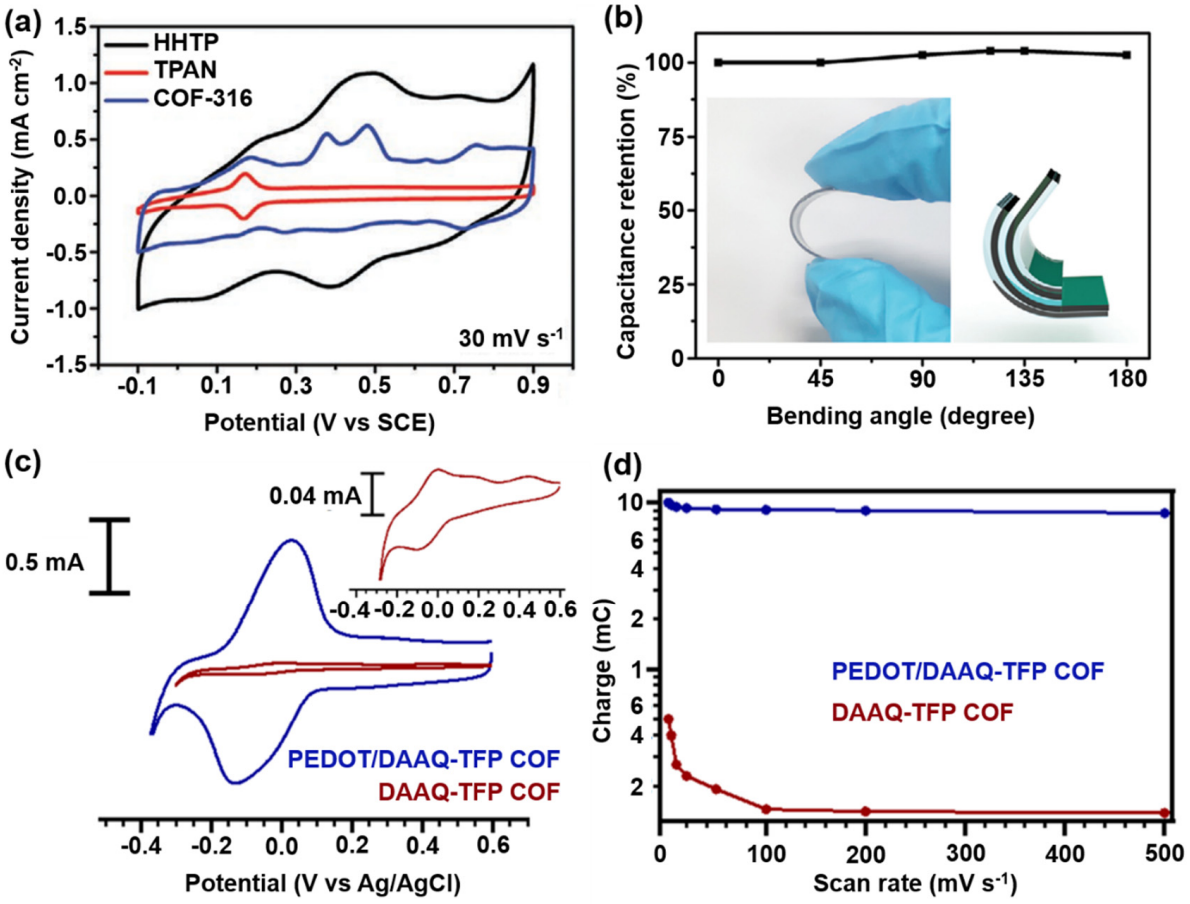

Figure 3. Electrochemical performance enhancement via the post synthetic modification strategy.

(**a**) CV curves of COF–316, HHTP, and TPAN at the scan rate of 30 mV s^{-1}. (**b**) The capacitance retention curves of COF–316–1@PPy FTCEs under various bending angles of 0°, 45°, 90°, 120°, 135°, 150°, and 180° at 50 mV s^{-1}. Inset: The photograph and sketch map of the TFSCs under bending [52]. Copyright 2021, Wiley-VCH. (**c**) CV response at 20 mV s^{-1} in 0.5 M H_2SO_4 of a PEDOT-modified DAAQ–TFP film, 1 μm-thick (blue), and the same as-synthesized DAAQ–TFP film before EDOT polymerization (red). The inset presents the cyclic voltametric response for the unmodified film using an expanded current scale. (**d**) The integrated charge associated with the oxidative wave of a PEDOT-modified DAAQ–TFP COF film (blue) and unmodified DAAQ–TFP COF film (red) recorded over various scan rates indicate that the PEDOT-modified films store more charge and tolerate faster scan rates than the unmodified films [53]. Copyright 2016, American Chemical Society.

Surface Doping

Surface doping modification of COF crystals is also an important way to improve the conductivity. More flexible and positively charged organic linkers containing other parts can effectively coordinate with coordination functional groups. These organic linkers can enhance energy matching with ligand orbital overlap by forming a continuous delocalized charge pathway. In particular, materials containing azo ligands (including nitrogen) exhibit high electrical conductivity.

At present, the engineering of conductivity modification of COFs used in MEES is a very new topic, so in this section, a modification of MOF conductivity is taken as an example. In view of the inherent poor conductivity of organic frames, He et al. used the receptor molecular doping strategy to adjust the conductivity of organic frame thin film electrodes [55]. After doping with 7,7,8,8-tetracyanoquinododimethane (TCNQ), its overall conductivity increased 40 times, and the specific area capacitance of the micro-supercapacitor devices was up to 95.1 mF cm^{-2} (Figure 4b). In addition, the modified material continues its excellent flexibility, indicating that its molecular doping strategy can well customize the electronic properties of organic framework materials used for energy storage and conversion. As a result, this work can open up a brand new way for scholars to modify the conductivity of COFs used in MEES.

Similarly, the synthesized COF is doped to make the bad orbital overlap between organic ligands in COF form conductive channels under the action of redox-active guest molecules, so as to enhance the conductivity of non-conductive COFs [56]. Meng and his co-workers synthesized c-COF by using 2,3,9,10,16,17,23,24-octa-aminophthalocyanine nickel (II) and pyrene-4,5,9,10-tetraone (Figure 4c) [57]. Its intrinsic conductivity is 2.51 × 10^{-3} S m^{-1}. This c-COF was then doped with the previously reported I_2 dopant, increasing its conductivity by another three orders of magnitude [58–61]. Similarly, Yang et al. grew a layer of COF film in situ on the substrate under solvothermal conditions, and the conductivity increased by four orders of magnitude after doping with iodine, because the anisotropic carrier transport in the frame was conducive to the transfer of out-of-plane holes [62]. At the same time, this conductive columnar stacked COF has good electrochemical performance, with a long cycling performance (Figure 4d) and a normalized capacitance of 19 μF cm^{-2}. In general, post-synthetic modification can improve the conductivity of COF without destroying the original properties, which is a very promising strategy in conductivity modification [53,63,64].

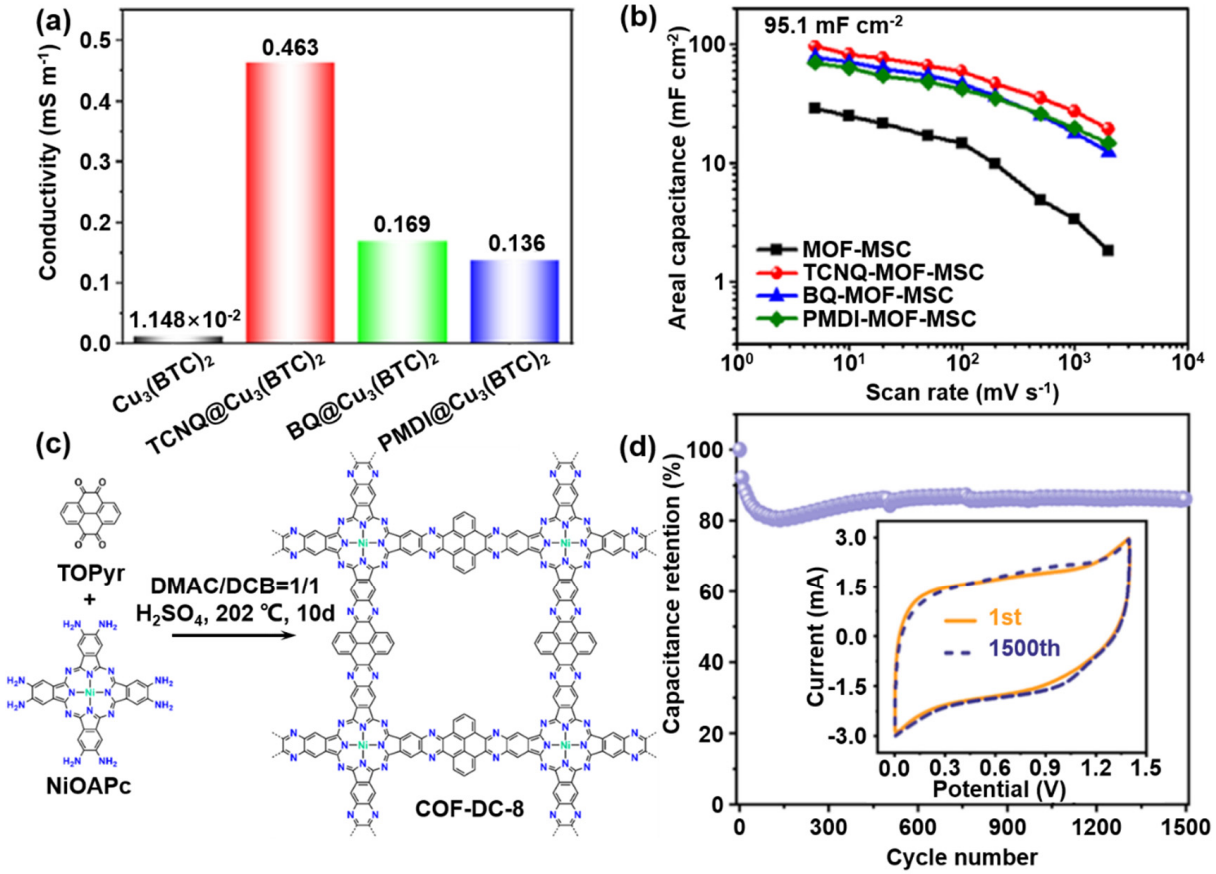

Figure 4. Surface conductivity modification on electrochemical performance. (**a**) Electrical conductivities of the $Cu_3(BTC)_2$, TCNQ@$Cu_3(BTC)_2$, BQ@$Cu_3(BTC)_2$, and PMDI@$Cu_3(BTC)_2$ thin films. (**b**) Specific capacitances calculated from CV curves as a function of scan rate [55]. Copyright 2020, Wiley-VCH. (**c**) Synthetic Route for 2D Conductive COF–DC–8 [57]. Copyright 2019, American Chemical Society. (**d**) Cycling stability test at 80 mV s^{-1}. Inset: comparison of initial and 1500th CV curve [62]. Copyright 2021, American Chemical Society.

2.2. Theoretical Assistances Explanation

The high speed and high efficiency of numerical algorithms are always the goals of people. Theoretical simulation has become an important method for accelerating the experimental cycle and reducing experimental consumption in view of the large number of ligands used to prepare COF and the difficulty in explaining its conductivity modification. Density functional theory can accurately simulate the interaction between COF molecules, intuitively prove the path of electron or proton migration, and better guide the conductivity modification strategy of COF. In addition, molecular dynamics simulation can simulate c-COFs on a large scale, which plays a guiding role in the synthesis and application of COFs. The factors of the COF conductivity modification strategy are analyzed from the perspectives of density functional theory and molecular dynamics simulation.

2.2.1. Density Functional Theory

Density functional theory (DFT) is a representative theoretical simulation method, which is widely used to simulate various properties of COFs, including hydrogen storage capacity [65], stacking mode [66,67], catalytic performance [68], and most importantly, electrical conductivity. As one of the most intuitive and accurate simulation methods for complex conductivity analysis, DFT is widely used [69], especially in COF ligands with many complex bonds and spatial arrangements. It has been reported in the past that organic polymers can conduct electrons both through bonds and through space, and

their correctness has been confirmed by DFT [70–72]. At the same time, the continuous overlap of molecular π-orbitals in COF contributes to charge transfer, and a large number of conjugated structures make π-π interactions between organic ligands easy to form, which has great potential for opening the direction of COF conductivity modification. In addition, some 2D COFs are capable of forming A-A stacks and have also been shown to readily form electron pathways [73–76].

On this basis, the researchers conducted simulation analysis of COFs, revealing the preference for atomic configuration. It is found that the A-A stack structure is the most stable among all COF structures (Figure 5a), which is in good agreement with the results obtained by morphology characterization [77]. However, the embedment of alkali-metal ions leads to a meta-stable state and tends to increase the torsion angle to stabilize the structure. In addition, the simulation also shows that the existence of nitrogen functional groups can further increase the alkali-metal ion storage capacity of the material, which is expected to increase the electrical conductivity of the material [78,79].

For COFs used in electrochemical energy storage devices, DFT simulation is the best choice considering both time and efficiency, and a large number of studies have been carried out in this area [80–82]. Wolfson and Schkeryantz used DFT to analyze the potassium ion storage capacity of 1,3,5-tris(arylethynyl)benzene and dehydrobenzoannulene ligands and found that the presence of alkynyl units could promote the binding of potassium ions with ligands. Thus, the potassium storage capacity of the electrode material is increased (Figure 5b) [83]. At the same time, the extended linear structure and the flexibility of the frame offer the possibility of accommodating more potassium ions. He et al. synthesized a COF that overlaps the direction of the *p*-column preferentially, which can provide a convenient transport channel for ions and electrons, and showed excellent electrochemical performance of 486.3 F g^{-1} [84]. Importantly, the DFT simulation results showed that the COF has low orbital localization, a narrow bandgap, and a low electron transport energy barrier, which fully explains its good electrical conductivity and provides a new choice for MEES device materials.

2.2.2. Molecular Dynamics

Since the density functional theory simulation needs to take into account every atom of COF, its volume cannot support multi-molecular simulation, which often requires an extremely long time to get results. Molecular dynamics is therefore a good choice for large-scale simulations. In general, in order for the microscopic simulation system to reflect the macroscopic experimental phenomenon, periodic boundary conditions are needed to replicate the simulated object system periodically to avoid the edge effect that does not exist in practice. In principle, for any particle system, the time-dependent Schrodinger equation needs to be solved, but in practical work, it pays more attention to the motion trajectory of the nucleus, and the Born–Oppenheimer approximation is used to solve the classical mechanical motion equation. This greatly reduces the difficulty of calculation, in order to efficiently obtain the properties of the whole system in a specific environment.

Similarly, for COFs, a single molecule cannot reveal the macroscopic physicochemical properties shown as an aggregate. In recent years, much work has been conducted to study the molecular dynamics of COF multi-molecular systems. Cuniberti et al. used classical molecular dynamics simulations to study the behavior of COF ligands at the air-water interface and analyzed in depth the advantages of liquid-gas interface synthesis of COF to improve the quality and control the properties of the synthesized materials (Figure 5c) [85]. It was found that the presence of water promoted the angular rotation of azine dihedral to the planar configuration, which was more favorable for the synthesis of 2D COF and the polymerization of large-area COF monolayers. In addition, molecular dynamics can well simulate the properties of membrane surfaces. Recent simulation studies show that in regulating the hydrophilicity of the film, the pre-deposited COF layer can slow down the diffusion rate of the reaction interface by hydrogen bonding, thus, reducing the thickness of the film and avoiding the formation of interface defects (Figure 5d) [86].

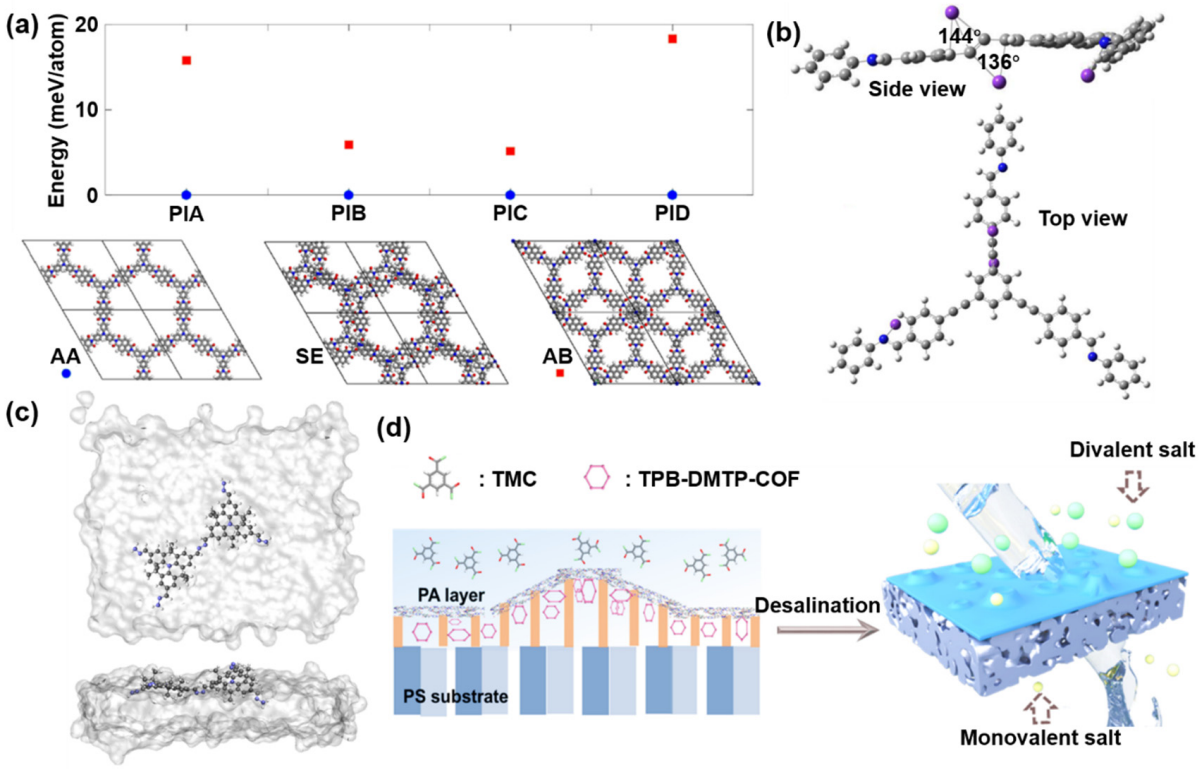

Figure 5. Theoretical assistances explanation for conductive COFs. (**a**) Energy difference between the AA eclipsed, AB staggered stacking for the four COFs, an illustration of the AA eclipsed, AB staggered and an example of serrated stacking (SE) [77]. Copyright 2021, American Chemical Society. (**b**) Visualization of optimized geometry of three potassium ions bound to radical anionic TAEB-PI [83]. Copyright 2021, American Chemical Society. (**c**) Top and lateral views of the final configuration of the azine-linked BTPHA1 dimer at the air-water interface by using DFTB MD simulations [85]. Copyright 2021, American Chemical Society. (**d**) Mechanism of the separation process of the COF-modulated thin-film nano-composite membrane [86]. Copyright 2022, American Chemical Society.

In summary, molecular dynamics has unique advantages in the preparation and application of COFs. Unfortunately, there are few reports on the application of molecular dynamics simulation of COF in MEES. However, this simulation method has a very broad prospect for the performance improvement of MEES devices by COF.

3. Synthesis Strategies of Organic Frameworks

The synthesis of COF is to covalently combine organic ligands into a designed frame structure, which has strict requirements on the reaction environment (such as temperature, solvent, and pressure), synthesis parameters (such as time and catalyst), and reaction steps. Small differences can lead to product differences in morphology, porosity, and other aspects. In general, top-down and bottom-up strategies are two defined synthesis strategies [87,88]. In this section, we give a brief overview of both strategies and discuss the advantages and disadvantages of each approach.

3.1. Top-Down Strategy

The basic methods of the top-down strategy include the wet chemical method and the liquid phase stripping method. The main principle is that the bulk material is dispersed in the solvent and then degraded by sound waves. The generated bubbles will be accompanied by micro-jet and vibration waves in the process of bursting, and concentrated tensile stress will be generated between the layers of bulk material to assist stripping.

The COF monolayer membrane structure has full application prospects in filtration, screening, and energy in terms of ion permeability, selectivity, and order. Since molecules

in COF crystals are bound together only by hydrogen bonds or van der Waals forces, the monolayer structure of COF can be obtained by simple mechanical, ultrasonic, and chemical-mediated stripping [89,90]. This top-down preparation method results in materials that retain their original crystal properties, such as pore structure, electrical conductivity, and ionic affinity. Li and Zhang prepared porous COF-1 nano-sheets by the ultrasonic stripping method, and their excellent permeability, inherent porosity, and strong covalent bond gave them great advantages in molecular screening [91]. David W. Burke and his collaborators used acid-mediated reactivation of imine bonds in COF to partially dissociate COF particles and eventually repolymerize uniformly on the membrane, resulting in a highly crystallized and mechanically good membrane structure (Figure 6a,b) [92]. This strategy of using acid to strip COFs could open up a number of potential applications for such materials that were previously unrealized.

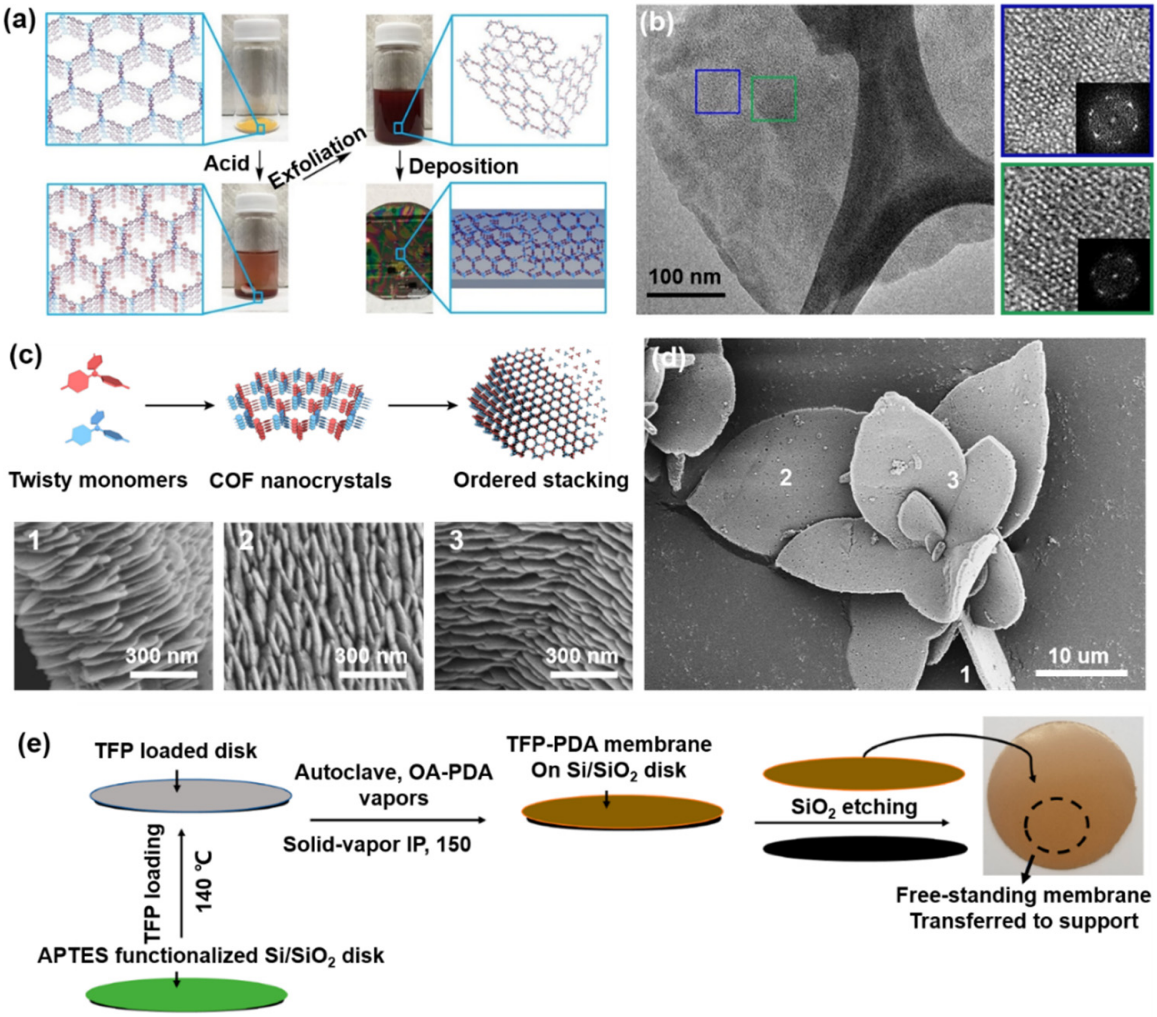

Figure 6. Specific COF structures can be constructed via different synthesis strategies. (**a**) Overview of the acid-exfoliation and film-casting procedures. (**b**) HRTEM image of an exfoliated BND–TFB COF sheet [92]. Copyright 2019, Wiley-VCH. (**c**) Schematic illustration of employing twisty monomers to achieve ordered stacking for producing long-range ordered COF assemblies. (**d**) FESEM images of flower-shaped TAPA–TFPA COF assemblies at different scales [93]. Copyright 2021, American Chemical Society. (**e**) Solid-vapor IP for the TFP–PDA membrane, including membrane growth and HF etching step to obtain free-standing membrane [94]. Copyright 2020, American Chemical Society.

The top-down preparation method can obtain thin-layer COFs without destroying the original morphology and can easily prepare COFs suitable for different application environments. However, the huge material waste caused by it cannot be ignored, and there

are still defects and deficiencies in the regulation of the distance between atoms and ions. Most importantly, the 2D COF ligand reduces the specific surface area of the material during the stripping process by eliminating the need for stacking and creating amorphous linked polymers, resulting in a loss of catalytic, molecular screening, and energy storage properties. Therefore, new preparation methods need to be explored and innovated by scholars.

3.2. Bottom-Up Strategy

A bottom-up strategy means that before synthesizing a COF, functional groups with functions are connected to structural units, and then react with other structural units, so that the functionalized groups can be evenly distributed in COFs, and the position of active sites on COFs can be accurately controlled. Several methods can be classified as bottom-up strategies, such as chemical vapor deposition (CVD), PLD, and spray coating [95].

General materials are usually prepared by acid etching or electron beam etching, which are of high cost and low efficiency and cannot be produced on a large scale. The bottom-up method mainly uses chemical synthesis to assemble organic small molecules into large-area COFs [96,97]. Therefore, bottom-up self-assembly technology provides the possibility for large-scale manufacturing of homogeneous COFs, but direct assembly through small molecules remains a challenge. Wang et al. demonstrated that the synthesis of conductive 2D COFs can be carried out directly in solution, and directly self-assembled into nano-scale or higher polymer structures by polycondensation of monomers with COF ligand structures (Figure 6c,d) [93]. This is rare in previous work, because the poor reversibility of covalent bonds leads to irregular monomer connections, and strong molecular interactions lead to disordered stacking between 2D molecules [98–100].

In addition, it is possible to prepare COF easily and efficiently by bottom-up direct synthesis with the interface method. Generally speaking, the liquid-liquid interface formed between two insoluble liquids is a more reliable preparation method [101–103]. In further studies, it was found that the diffusion rate of the gas-phase molecule was superior to that of the liquid-phase monomer molecule, resulting in the synthesis efficiency at the gas-solid interface being eight times that of the traditional liquid-liquid interface [94]. At the same time, the stable gas-solid interface is beneficial for increasing the reaction temperature, increasing the diffusion rate of the monomer, and further accelerating the reaction rate of the COF two-phase monomer (Figure 6e). This work creates a new method of interface preparation beyond the liquid-liquid interface and provides a basis for a new bottom-up interface preparation method. In conclusion, bottom-up synthesis is a good choice for the simple and efficient synthesis of long-range ordered meta-structure COFs by self-assembly at a molecular scale.

In general, the synthesis of COF has a unique design principle, which can be prepared by two different synthesis methods: bottom-up and top-down. Top-down synthesis methods have been proven to be stable in the synthesis of materials over a long period of time, including etching, stripping, and other traditional methods, but the yield of the final product needs to be considered. Homogeneous products can be prepared with high efficiency and low cost through bottom-up self-assembly of small molecules, including direct synthesis, inter-facial synthesis, and other methods. The two methods have their own advantages and disadvantages, so many factors should be considered in COF design and an appropriate manufacturing strategy should be selected.

4. Design Criteria for Conductive COF Applied to MEES

Due to their unique physical and chemical properties, c-COFs have broad application prospects in the electrochemical field [104–107]. For the electrode materials used in electrochemical energy storage devices, it is necessary to have a material with high adaptability to ion de-embedding, fast ion-electron conduction path, and high density of active sites. In recent years, much research has been devoted to promoting the development of COFs in this field, and many achievements have been achieved [27,108–111]. Compared with MOF, COF excludes the unwanted orbital overlap between the p-orbital of an organic ligand and

the d-orbital of a metal ion, which gives a lot of inspiration to COFs and arouses the interest of scholars [112]. Additionally, COFs are composed of light elements (such as C, O, H, and N) connected via covalent bonds, which avoids the potential toxicity and environmental pollution caused by heavy metals in MOFs [113]. In addition, when used as MEES electrode materials, the crystal structure of MOF-based materials collapses during charging and discharging, while the COF with elastic bond structure provides the possibility to adapt to volume changes [114,115]. Specifically, COF can be used in new electrochemical energy storage systems for the following reasons and characteristics.

4.1. Good Pore Distribution

According to most reports, porous frame structures are characterized by the high density of COF reaction sites, modified skeletons, and high pore structures. These characteristics enable active substances to be fully impregnated within the COF framework channels, to better selectively adsorb gases or ions, and, more importantly, to improve electrochemical reaction efficiency. Yang et al. took advantage of the uniform pore environment and high pore density of COF to apply COF to monolayer membranes in osmotic power generation and achieved an output power of more than 200 W m^{-2} (Figure 7a,b) [116]. If c-COF can be fully utilized with a well-ordered pore arrangement, low resistivity, and ultra-high ionic conductivity, it can also perform surprisingly well on MEES devices. In addition, the good pore structure improves the intrinsic specific surface area of the material and has high chimerism with electrolyte molecules, effectively accelerating ion and electron migration.

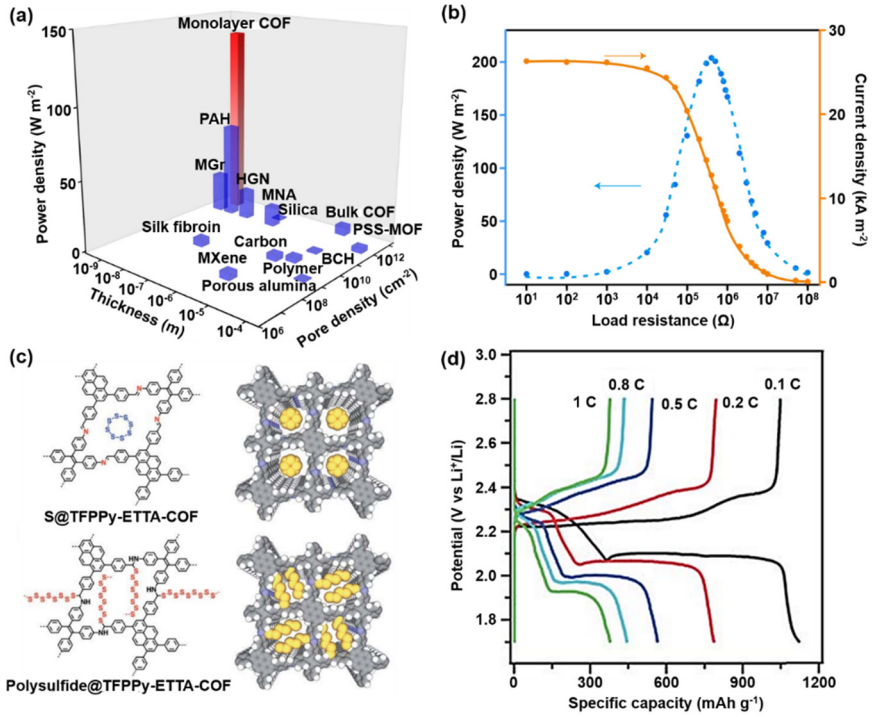

Figure 7. Enhancement of electrochemical performance by good pore structure and aligned channels. (**a**) Comparison of the osmotic power-generation performance of the COF monolayer membrane with state-of-the-art results from the literature in terms of membrane thickness, pore density and output power density. (**b**) Current density and output power density dependence on the external load resistance on mixing artificial seawater with artificial river water [116]. Copyright 2022, Springer Nature. (**c**) Physical isolation of sulfur (S_8 ring) in the COF and covalent engineering of polysulfide chains on the pore walls. (**d**) Charge-discharge curves of polysulfide@TFPPy–ETTA–COF at different rates [117]. Copyright 2019, The Royal Society of Chemistry.

4.2. Aligned Channels

For two-dimensional (2D) and three-dimensional (3D) COFs, the interaction between their specific organic ligands promotes the formation of COF channels [118]. The columnar structure formed by the stacking of aromatic groups in the 2D COF provides a transport path for electrons and ions. The inter-weaving of the medium and short conjugated groups in the 3D COF and the establishment of a growth-order conjugated system is also a good transport path. This channel promotes the transport of electrons and ions, and reduces the inherent transport resistance between ligands, and facilitates the transport of electrons and ions to the deep reactive sites, thus, improving the overall utilization rate of COFs. For example, TFPPy–ETTA–COF materials with one-dimensional (1D) channels provide good carrier space for polysulfides (Figure 7c). The resulting COF has a high sulfur load, high speed, and cycle stability, which has great application potential in lithium-sulfur batteries (Figure 7d) [117].

4.3. Dynamic Reversible Crystal Structure

The organic ligands in COF are connected by covalent bonds, while the conjugated organic groups condense the long-chain organic carbon structure by specific arrangement. This structure is strongly covalently binding in the axial direction, but malleable in the normal direction. Therefore, in the process of ion deintercalation, the material has properties similar to respiration, which can well adapt to volume change and has high cyclic stability in the electrochemical energy storage system. In addition, the malleability of COF also enables it to be studied for flexible devices, especially for flexible MEES devices with wide application prospects.

In 2017, Ma et al. analyzed the structural transformation and dynamic behavior of 3D COF (Figure 8a), revealing that –C=N– can be used as the design idea for dynamic COF [119,120]. On this basis, Liu et al. successfully designed an FCOF–5 material with flexible and reversible expansion and contraction during adsorption and desorption (Figure 8b) and proved the important role of –C–O– in its respiration [121].

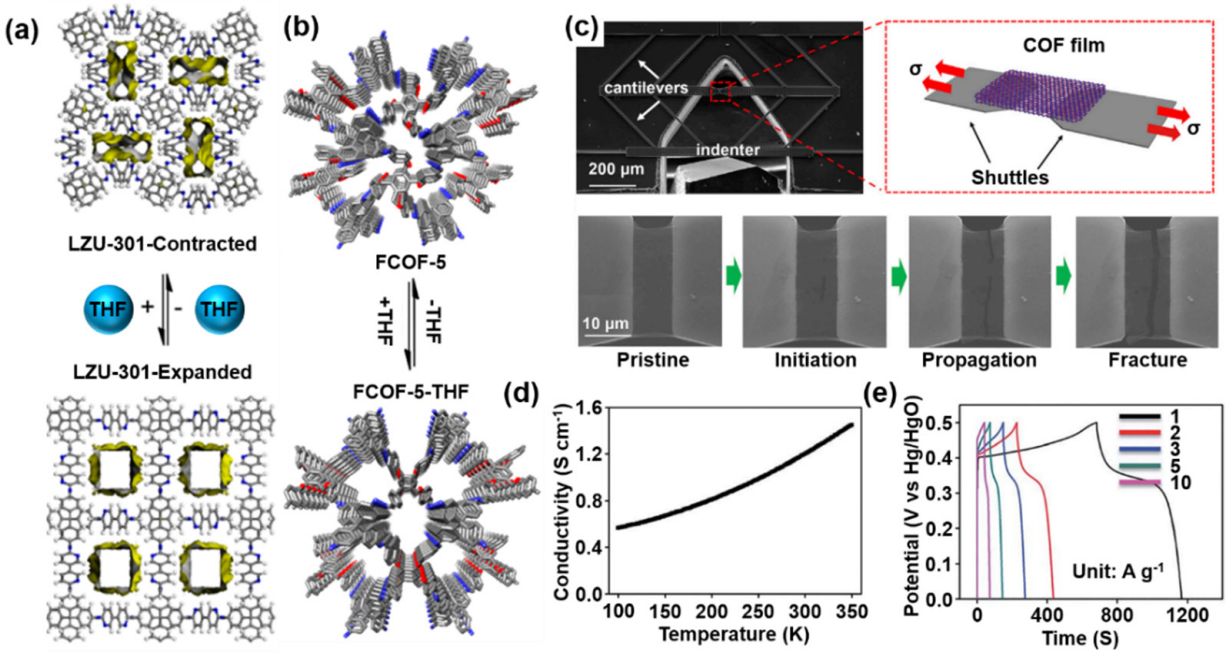

Figure 8. Optimization of dynamic structure, mechanical properties, and electrochemical activity for MEES devices. (**a**) Schematic illustration of the transformation into the expanded structure presented in LZU–301 [119]. Copyright 2017, American Chemical Society. (**b**) Reversible crystal

structures transformation between FCOF–5 and FCOF–5–THF [121]. Copyright 2021, American Chemical Society. (**c**) SEM image and schematic for uniaxial tension of nano-mechanical devices (above). In situ tensile snapshots of the COF film with the whole process of crack propagation (below) [120]. Copyright 2021, Elsevier Inc. (**d**) Variable-temperature van der Pauw conductivity measurement. (**e**) GCD curves at different current densities (1–10 A g^{-1}) [122]. Copyright 2019, The Royal Society of Chemistry.

4.4. Excellent Mechanical Properties

Good pore and channel structure, and more importantly, excellent flexibility and ductility, are the pre-conditions for good adaptability in MEES devices. In previous works, 2D COFs provide mechanical properties that are not available in conventional 2D materials [123–125]. In order to evaluate the planar mechanical properties of 2D COFs, Fang et al. studied the tensile mechanical behavior of CoFTAPb–DHTA films (Figure 8c). Quantitative in situ SEM tests were used to study the tensile mechanical properties and fracture behavior of COF films [120]. It is found that the 2D COF has excellent performance in fracture strength and fracture toughness (~1.3 times that of graphene) and has insensitivity to cracks. This property enables 2D COFs to maintain electrode integrity when applied to MEES devices under morphological changes.

4.5. Electrochemical Activity

In addition to the above features, reversible electrochemical reaction and reduction are other important features of COF. As a promising electrochemical material for MEES, conducting COF has a variety of characteristics, such as high density of exposed active sites, large specific surface area, stable chemical properties, and conductivity. Therefore, the application of c-COFs in the field of energy storage has been widely studied in recent years (Table 1) [126]. For example, a 2D Ni–COF with ultra-high conductivity (compared to other COFs) and a large calculated specific surface area is used as an electrode material in supercapacitors (Figure 8d) [122]. This 2D c-COF with square planar bivalent Ni coordination has a highly conjugated skeleton, an ordered porous structure, and a large number of redox centers, resulting in a high specific capacitance of 1257 F g^{-1} in supercapacitors. In addition, its high conductivity compared to other COFs enables it to achieve satisfactory results in long cycles. In particular, its excellent conductivity comes from the coordination of planar bivalent Ni and the combination of the Ni-Salphen unit with *p*-conjugate. Therefore, its high conductivity and large number of active sites significantly improve its capacitance and cycling stability as an electrode material for MEES devices (Figure 8e). COF materials often exhibit impressive electrochemical properties, especially huge specific capacities and large energy densities, much higher than current conventional electrode materials [127–131].

Table 1. COF-derived electrode materials and their electrochemical performance.

COFs	BET (m^2 g^{-1})	Pores Size (nm)	Specific Capacitance	Power Density	Energy Density	Capacity Retention	Application	Ref.
Tf–TAPA	159.55	1.47			583 mAh g^{-1} at 2 A g^{-1}	96% (1500) at 8 A g^{-1}	LIBs	[132]
AAm–TPB	403	2.99	271 F g^{-1} at 1 A g^{-1}	19.16 Wh kg^{-1} at 350 W kg^{-1}		92% (10,000) at 5 A g^{-1}	ASCs	[133]
AZO–1	649	2.8		2800 W kg^{-1}	140 mAh g^{-1} at 0.5 C	(5000) at 10 C	LIBs	[134]
COF–316@PPy	452	1.56	783.6 μF cm^{-2} at 3 μA cm^{-2}			100% (3400) at 20 μA cm^{-2}	ASCs	[52]
g–$C_{34}N_6$–COF	1003		15.2 mF cm^{-2} at 2 mV s^{-1}	7.3 mWh cm^{-3} at 50 mW cm^{-3}		93.1% (5000)	ASCs	[30]
e-COFs	1170	3.4	5.46 mF cm^{-2} at 1000 mV s^{-1}	1002 mW cm^{-3} at 0.23 mWh cm^{-3}		100% (10,000)	EDLCs	[135]
DAAQ–COFs/GA	425.3	1.77	378 F g^{-1} at 1 A g^{-1}	30.5 Wh kg^{-1} at 700 W kg^{-1}		88.9% (20,000) at 5 A g^{-1}	ASCs	[136]
AQ–COF@CNTs	905				144 mAh g^{-1} at 50 mA g^{-1}	100% (3000) at 250 mA g^{-1}	LIBs	[137]
c-CNT@COF–3	576.7	1.5	418.7 F g^{-1} at 0.2 A g^{-1}	30.7 mWh cm^{-2} and 591.9 mW cm^{-2}		94% (10,000) at 10 mA cm^{-2}	ASCs	[138]
TpPa–COF@PANI	574	1.3	95 F g^{-1} at 0.2 A g^{-1}			83% (30,000) at 5 A g^{-1}	ASCs	[139]

5. Conclusions and Outlook

The increasing demand for the miniaturization of electronic devices has stimulated the research on electrochemical storage devices. In order to maintain the electrochemical performance of micro-energy storage devices under the premise of reducing the scale, a kind of electrode material that can meet the special requirements of MEES and has high performance is needed. C-COF has a good application prospect in MEES due to its high conductivity, excellent pore distribution, regular migration channel, and good mechanical properties. In this paper, the conductive modification strategy, preparation strategy, and the latest research progress of COF in MEES devices are reviewed. C-COF provides great opportunities for the development of MEES devices, but the field is still in the preliminary stage of exploration and will face many challenges to be solved.

Although preliminary studies show great promise for conducting COF in MEES electrodes, there are still great challenges in practical application. The conductivity of c-COF has a huge increase in the order of magnitude, but compared with mature electrode materials, its conductivity has a large catch-up space. Generally speaking, adding a sufficient amount of conductive agent can improve the utilization efficiency of c-COF, but this method will reduce the specific mass capacity of the electrode material, which has a great impact on the performance of MEES devices. Therefore, the design of a non-conductive and non-adhesive MEES electrode will be an excellent solution. At the same time, as more and more COFs are developed by scholars, a huge database is gradually forming. With the upgrading of algorithms and the rapid improvements in computing power in computational materials science, high-throughput computational screening and machine learning have become a rapidly targeted experimental strategy. Such research could accelerate the development of novel COFs for use in special MEES devices. It is foreseeable that, in the near future, theoretical simulation will guide experimental research, accurately regulate the structure of COF, and effectively utilize the performance of COF in all aspects.

It has been proven in many studies that the conductivity of 2D COFs is usually better than that of 3D COFs. The reason is that 2D COF with limited layers can reduce the migration distance of ions and electrons in a 2D plane and promote the diffusion of ions and electrons. At the same time, the ordered A-A stack structure can allow ions and electrons to move freely between layers, and the nitrogen-rich functional groups can enhance electrical conductivity. However, the preparation process of 2D COF is more difficult than that of 3D COF. Three-dimensional COF is generally synthesized from the bottom-up with the simple solvothermal method without considering the complex 2D stack structure. On the contrary, if the bottom-up method is used to prepare 2D COF, it needs extremely stringent conditions, which is contrary to large-scale commercialization. In addition, the size, crystallinity, and stacking mode of block COF on the kinetics of stripping still need to be further investigated. Therefore, careful consideration is necessary for the design of COF before synthesis.

Other energy storage systems should also be considered by MEES, including micro-lithium sulfur batteries, micro-lithium air batteries, etc. It is always the goal to maximize the performance of c-COFs. In addition, future work should not be limited to the electrochemical storage of alkali-metal ions. For polyvalent ions, c-COF electrode materials have a lot of scope for research, but they also face additional challenges. We believe that c-COF can lead the development of post-lithium energy storage and has better application in the latest MEES branch.

Author Contributions: C.Q.: Investigation, Visualization, Writing—original draft. R.W.: Methodology, Writing—original draft, Writing—review and editing. F.Y.: Conceptualization, Supervision, Writing—review and editing. K.S.: Conceptualization, Writing—review and editing. J.L.: Conceptualization, Supervision, Writing—review and editing. W.B.: Conceptualization, Investigation, Visualization, Writing—review and editing. C.G.: Conceptualization, Supervision, Writing—review and editing. H.L.: Conceptualization, Supervision, Writing—review and editing. All authors have read and agreed to the published version of the manuscript.

Funding: The work was supported by the National Natural Science Foundation of China (No. 22005150), the Natural Science Foundation of Jiangsu (No. BK20200825), and the Jiangsu Provincial Scientific Research and Practice Innovation Program (No. KYCX22_1191). W.B. also acknowledges the financial support of the Startup Foundation for Introducing Talent of NUIST.

Institutional Review Board Statement: Not applicable.

Informed Consent Statement: Not applicable.

Data Availability Statement: Not applicable.

Conflicts of Interest: The authors declare that they have no known competing financial interests or personal relationships that could have appeared to influence the work reported in this paper.

References

1. Miskin, M.Z.; Cortese, A.J.; Dorsey, K.; Esposito, E.P.; Reynolds, M.F.; Liu, Q.; Cao, M.; Muller, D.A.; McEuen, P.L.; Cohen, I. Electronically integrated, mass-manufactured, microscopic robots. *Nature* **2020**, *584*, 557–561. [CrossRef]
2. Wang, R.; Sun, K.; Zhang, Y.; Qian, C.; Bao, W. Dimensional optimization enables high-performance capacitive deionization. *J. Mater. Chem. A* **2022**, *10*, 6414–6441. [CrossRef]
3. Wang, R.; Li, M.; Sun, K.; Zhang, Y.; Li, J.; Bao, W. Element-Doped Mxenes: Mechanism, Synthesis, and Applications. *Small* **2022**, *18*, e2201740. [CrossRef] [PubMed]
4. Wang, R.; Sun, K.; Zhang, Y.; Li, B.; Qian, C.; Li, J.; Liu, F.; Bao, W. Nanoscale interface engineering of inorganic Solid-State electrolytes for High-Performance alkali metal batteries. *J. Colloid Interface Sci.* **2022**, *621*, 41–66. [CrossRef]
5. Bao, W.; Wang, R.; Qian, C.; Zhang, Z.; Wu, R.; Zhang, Y.; Liu, F.; Li, J.; Wang, G. Porous Heteroatom-Doped $Ti_3C_2T_x$ MXene Microspheres Enable Strong Adsorption of Sodium Polysulfides for Long-Life Room-Temperature Sodium-Sulfur Batteries. *ACS Nano* **2021**, *15*, 16207–16217. [CrossRef] [PubMed]
6. Bao, W.; Wang, R.; Li, B.; Qian, C.; Zhang, Z.; Li, J.; Liu, F. Stable alkali metal anodes enabled by crystallographic optimization—A review. *J. Mater. Chem. A* **2021**, *9*, 20957–20984. [CrossRef]
7. Li, J.; Liu, H.; Sun, K.; Wang, R.; Qian, C.; Yu, F.; Zhang, L.; Bao, W. Dual-functional iodine photoelectrode enabling high performance photo-assisted rechargeable lithium iodine batteries. *J. Mater. Chem. A* **2022**, *10*, 7326–7332. [CrossRef]
8. Wang, R.; Sun, K.; Liu, H.; Qian, C.; Li, M.; Zhang, Y.; Bao, W. Integrating a Redox-Coupled $FeSe_2$/N-C Photoelectrode into a Potassium Ion Hybrid Capacitors for Photoassisted Charging. *J. Mater. Chem. A* **2022**, *10*, 11504–11513. [CrossRef]
9. Qian, C.; Sun, K.; Bao, W. Recent advance on machine learning of MXenes for energy storage and conversion. *Int. J. Energy Res.* **2022**. [CrossRef]
10. Shi, X.; Das, P.; Wu, Z.-S. Digital Microscale Electrochemical Energy Storage Devices for a Fully Connected and Intelligent World. *ACS Energy Lett.* **2021**, *7*, 267–281. [CrossRef]
11. Xu, T.; Du, H.; Liu, H.; Liu, W.; Zhang, X.; Si, C.; Liu, P.; Zhang, K. Advanced Nanocellulose-Based Composites for Flexible Functional Energy Storage Devices. *Adv. Mater.* **2021**, *33*, 2101368. [CrossRef] [PubMed]
12. Yue, X.; Johnson, A.C.; Kim, S.; Kohlmeyer, R.R.; Patra, A.; Grzyb, J.; Padmanabha, A.; Wang, M.; Jiang, Z.; Sun, P.; et al. A Nearly Packaging-Free Design Paradigm for Light, Powerful, and Energy-Dense Primary Microbatteries. *Adv. Mater.* **2021**, *33*, e2101760. [CrossRef] [PubMed]
13. Yu, D.; Goh, K.; Wang, H.; Wei, L.; Jiang, W.; Zhang, Q.; Dai, L.; Chen, Y. Scalable synthesis of hierarchically structured carbon nanotube–graphene fibres for capacitive energy storage. *Nat. Nanotechnol.* **2014**, *9*, 555–562. [CrossRef] [PubMed]
14. Kyerematen, N.A.; Brousse, T.; Pech, D. Microsupercapacitors as miniaturized energy-storage components for on-chip electronics. *Nat. Nanotechnol.* **2016**, *12*, 7–15. [CrossRef]
15. Chen, J.; Huang, Y.; Zhang, N.; Zou, H.; Liu, R.; Tao, C.; Fan, X.; Wang, Z.L. Micro-cable structured textile for simultaneously harvesting solar and mechanical energy. *Nat. Energy* **2016**, *1*, 16138. [CrossRef]
16. Zhou, F.; Huang, H.; Xiao, C.; Zheng, S.; Shi, X.; Qin, J.; Fu, Q.; Bao, X.; Feng, X.; Müllen, K.; et al. Electrochemically Scalable Production of Fluorine-Modified Graphene for Flexible and High-Energy Ionogel-Based Microsupercapacitors. *J. Am. Chem. Soc.* **2018**, *140*, 8198–8205. [CrossRef]
17. Zhang, J.; Zhang, G.; Zhou, T.; Sun, S. Recent Developments of Planar Micro-Supercapacitors: Fabrication, Properties, and Applications. *Adv. Funct. Mater.* **2020**, *30*, 1910000. [CrossRef]
18. Bao, W.; Wang, R.; Qian, C.; Li, M.; Sun, K.; Yu, F.; Liu, H.; Guo, C.; Li, J. Photoassisted High-Performance Lithium Anode Enabled by Oriented Crystal Planes. *ACS Nano* **2022**. [CrossRef]
19. Liu, Y.; Zhou, H.; Zhou, W.; Meng, S.; Qi, C.; Liu, Z.; Kong, T. Biocompatible, High-Performance, Wet-Adhesive, Stretchable All-Hydrogel Supercapacitor Implant Based on PANI@rGO/Mxenes Electrode and Hydrogel Electrolyte. *Adv. Energy Mater.* **2021**, *11*, 2101329. [CrossRef]
20. Wang, X.; Wu, Z. Zinc based micro-electrochemical energy storage devices: Present status and future perspective. *EcoMat* **2020**, *2*, e12042. [CrossRef]

21. Chang, Y.; Sun, X.; Ma, M.; Mu, C.; Li, P.; Li, L.; Li, M.; Nie, A.; Xiang, J.; Zhao, Z.; et al. Application of hard ceramic materials B4C in energy storage: Design B4C@C core-shell nanoparticles as electrodes for flexible all-solid-state micro-supercapacitors with ultrahigh cyclability. *Nano Energy* **2020**, *75*, 104947. [CrossRef]
22. Sun, N.; Zhou, D.; Liu, W.; Li, A.; Su, Y.; Jiang, P.; Zou, Y.; Shi, S.; Liu, F. Sputtered titanium nitride films with finely tailored surface activity and porosity for high performance on-chip micro-supercapacitors. *J. Power Source* **2021**, *489*, 229406. [CrossRef]
23. Shao, Y.; El-Kady, M.F.; Sun, J.; Li, Y.; Zhang, Q.; Zhu, M.; Wang, H.; Dunn, B.; Kaner, R.B. Design and Mechanisms of Asymmetric Supercapacitors. *Chem. Rev.* **2018**, *118*, 9233–9280. [CrossRef] [PubMed]
24. Rogge, S.M.J.; Bavykina, A.; Hajek, J.; Garcia, H.; Olivos-Suarez, A.I.; Sepúlveda-Escribano, A.; Vimont, A.; Clet, G.; Bazin, P.; Kapteijn, F.; et al. Metal–organic and covalent organic frameworks as single-site catalysts. *Chem. Soc. Rev.* **2017**, *46*, 3134–3184. [CrossRef]
25. Li, Y.; Karimi, M.; Gong, Y.-N.; Dai, N.; Safarifard, V.; Jiang, H.-L. Integration of metal-organic frameworks and covalent organic frameworks: Design, synthesis, and applications. *Matter* **2021**, *4*, 2230–2265. [CrossRef]
26. Keller, N.; Bein, T. Optoelectronic processes in covalent organic frameworks. *Chem. Soc. Rev.* **2020**, *50*, 1813–1845. [CrossRef]
27. Li, J.; Jing, X.; Li, Q.; Li, S.; Gao, X.; Feng, X.; Wang, B. Bulk COFs and COF nanosheets for electrochemical energy storage and conversion. *Chem. Soc. Rev.* **2020**, *49*, 3565–3604. [CrossRef]
28. Li, X.; Cai, S.; Sun, B.; Yang, C.; Zhang, J.; Liu, Y. Chemically Robust Covalent Organic Frameworks: Progress and Perspective. *Matter* **2020**, *3*, 1507–1540. [CrossRef]
29. Geng, K.; He, T.; Liu, R.; Dalapati, S.; Tan, K.T.; Li, Z.; Tao, S.; Gong, Y.; Jiang, Q.; Jiang, D. Covalent Organic Frameworks: Design, Synthesis, and Functions. *Chem. Rev.* **2020**, *120*, 8814–8933. [CrossRef]
30. Xu, J.; He, Y.; Bi, S.; Wang, M.; Yang, P.; Wu, D.; Wang, J.; Zhang, F. An Olefin-Linked Covalent Organic Framework as a Flexible Thin-Film Electrode for a High-Performance Micro-Supercapacitor. *Angew. Chem. Int. Ed.* **2019**, *58*, 12065–12069. [CrossRef]
31. Bi, S.; Yang, C.; Zhang, W.; Xu, J.; Liu, L.; Wu, D.; Wang, X.; Han, Y.; Liang, Q.; Zhang, F. Two-dimensional semiconducting covalent organic frameworks via condensation at arylmethyl carbon atoms. *Nat. Commun.* **2019**, *10*, 2467. [CrossRef] [PubMed]
32. Lyu, H.; Diercks, C.S.; Zhu, C.; Yaghi, O.M. Porous Crystalline Olefin-Linked Covalent Organic Frameworks. *J. Am. Chem. Soc.* **2019**, *141*, 6848–6852. [CrossRef] [PubMed]
33. Ma, X.; Scott, T.F. Approaches and challenges in the synthesis of three-dimensional covalent-organic frameworks. *Commun. Chem.* **2018**, *1*, 98. [CrossRef]
34. Jin, Y.; Hu, Y.; Zhang, W. Tessellated multiporous two-dimensional covalent organic frameworks. *Nat. Rev. Chem.* **2017**, *1*, 0056. [CrossRef]
35. Yusran, Y.; Li, H.; Guan, X.; Fang, Q.; Qiu, S. Covalent Organic Frameworks for Catalysis. *EnergyChem* **2020**, *2*, 100035. [CrossRef]
36. Li, B.; Zhao, Y.-M.; Kirchon, A.; Pang, J.-D.; Yang, X.-Y.; Zhuang, G.-L.; Zhou, H.-C. Unconventional Method for Fabricating Valence Tautomeric Materials: Integrating Redox Center within a Metal–Organic Framework. *J. Am. Chem. Soc.* **2019**, *141*, 6822–6826. [CrossRef]
37. Wang, D.-G.; Qiu, T.; Guo, W.; Liang, Z.; Tabassum, H.; Xia, D.; Zou, R. Covalent organic framework-based materials for energy applications. *Energy Environ. Sci.* **2020**, *14*, 688–728. [CrossRef]
38. Coropceanu, V.; Cornil, J.; da Silva Filho, D.A.; Olivier, Y.; Silbey, R.; Brédas, J.-L. Charge Transport in Organic Semiconductors. *Chem. Rev.* **2007**, *107*, 926–952. [CrossRef]
39. Ascherl, L.; Sick, T.; Margraf, J.T.; Lapidus, S.H.; Calik, M.; Hettstedt, C.; Karaghiosoff, K.; Döblinger, M.; Clark, T.; Chapman, K.W.; et al. Molecular docking sites designed for the generation of highly crystalline covalent organic frameworks. *Nat. Chem.* **2016**, *8*, 310–316. [CrossRef]
40. Mahmood, J.; Ahmad, I.; Jung, M.; Seo, J.-M.; Yu, S.-Y.; Noh, H.-J.; Kim, Y.H.; Shin, H.-J.; Baek, J.-B. Two-dimensional amine and hydroxy functionalized fused aromatic covalent organic framework. *Commun. Chem.* **2020**, *3*, 31. [CrossRef]
41. Yue, Y.; Li, H.; Chen, H.; Huang, N. Piperazine-Linked Covalent Organic Frameworks with High Electrical Conductivity. *J. Am. Chem. Soc.* **2022**, *144*, 2873–2878. [CrossRef] [PubMed]
42. Kang, C.; Zhang, Z.; Wee, V.; Usadi, A.K.; Calabro, D.C.; Baugh, L.S.; Wang, S.; Wang, Y.; Zhao, D. Interlayer Shifting in Two-Dimensional Covalent Organic Frameworks. *J. Am. Chem. Soc.* **2020**, *142*, 12995–13002. [CrossRef] [PubMed]
43. Wan, S.; Chen, Y.; Wang, Y.; Li, G.; Wang, G.; Liu, L.; Zhang, J.; Liu, Y.; Xu, Z.; Tomsia, A.P.; et al. Ultrastrong Graphene Films via Long-Chain π-Bridging. *Matter* **2019**, *1*, 389–401. [CrossRef]
44. Kim, S.Y.; Lee, J.; Park, M.J. Proton Hopping and Diffusion Behavior of Sulfonated Block Copolymers Containing Ionic Liquids. *Macromolecules* **2014**, *47*, 1099–1108. [CrossRef]
45. Wu, X.; Hong, J.J.; Shin, W.; Ma, L.; Liu, T.; Bi, X.; Yuan, Y.; Qi, Y.; Surta, T.W.; Huang, W.; et al. Diffusion-free Grotthuss topochemistry for high-rate and long-life proton batteries. *Nat. Energy* **2019**, *4*, 123–130. [CrossRef]
46. Zhao, Q.; Song, A.; Zhao, W.; Qin, R.; Ding, S.; Chen, X.; Song, Y.; Yang, L.; Lin, H.; Li, S.; et al. Boosting the Energy Density of Aqueous Batteries via Facile Grotthuss Proton Transport. *Angew. Chem. Int. Ed.* **2020**, *60*, 4169–4174. [CrossRef] [PubMed]
47. Yang, Y.; Zhang, P.; Hao, L.; Cheng, P.; Chen, Y.; Zhang, Z. Grotthuss Proton-Conductive Covalent Organic Frameworks for Efficient Proton Pseudocapacitors. *Angew. Chem. Int. Ed.* **2021**, *60*, 21838–21845. [CrossRef] [PubMed]
48. Meng, Z.; Aykanat, A.; Mirica, K.A. Proton Conduction in 2D Aza-Fused Covalent Organic Frameworks. *Chem. Mater.* **2018**, *31*, 819–825. [CrossRef]

49. Segura, J.L.; Royuela, S.; Ramos, M.M. Post-synthetic modification of covalent organic frameworks. *Chem. Soc. Rev.* **2019**, *48*, 3903–3945. [CrossRef] [PubMed]
50. Yusran, Y.; Guan, X.; Li, H.; Fang, Q.; Qiu, S. Postsynthetic functionalization of covalent organic frameworks. *Natl. Sci. Rev.* **2019**, *7*, 170–190. [CrossRef] [PubMed]
51. Wang, M.; Wang, M.; Lin, H.-H.; Ballabio, M.; Zhong, H.; Bonn, M.; Zhou, S.; Heine, T.; Cánovas, E.; Dong, R.; et al. High-Mobility Semiconducting Two-Dimensional Conjugated Covalent Organic Frameworks with *p*-Type Doping. *J. Am. Chem. Soc.* **2020**, *142*, 21622–21627. [CrossRef] [PubMed]
52. Wang, W.; Zhao, W.; Chen, T.; Bai, Y.; Xu, H.; Jiang, M.; Liu, S.; Huang, W.; Zhao, Q. All-in-One Hollow Flower-Like Covalent Organic Frameworks for Flexible Transparent Devices. *Adv. Funct. Mater.* **2021**, *31*, 2010306. [CrossRef]
53. Mulzer, C.R.; Shen, L.; Bisbey, R.P.; McKone, J.R.; Zhang, N.; Abruña, H.D.; Dichtel, W.R. Superior Charge Storage and Power Density of a Conducting Polymer-Modified Covalent Organic Framework. *ACS Central Sci.* **2016**, *2*, 667–673. [CrossRef]
54. Liu, M.; Chen, Y.J.; Huang, X.; Dong, L.Z.; Lu, M.; Guo, C.; Yuan, D.; Chen, Y.; Xu, G.; Li, S.L.; et al. Porphyrin-Based COF 2D Materials: Variable Modification of Sensing Performances by Post-Metallization. *Angew. Chem. Int. Ed.* **2022**, *61*, e202115308.
55. He, Y.; Yang, S.; Fu, Y.; Wang, F.; Ma, J.; Wang, G.; Chen, G.; Wang, M.; Dong, R.; Zhang, P.; et al. Electronic Doping of Metal-Organic Frameworks for High-Performance Flexible Micro-Supercapacitors. *Small Struct.* **2021**, *2*, 2000095. [CrossRef]
56. Wang, L.; Dong, B.; Ge, R.; Jiang, F.; Xu, J. Fluorene-Based Two-Dimensional Covalent Organic Framework with Thermo-electric Properties through Doping. *ACS Appl. Mater. Interfaces* **2017**, *9*, 7108–7114. [CrossRef]
57. Meng, Z.; Stolz, R.M.; Mirica, K.A. Two-Dimensional Chemiresistive Covalent Organic Framework with High Intrinsic Conductivity. *J. Am. Chem. Soc.* **2019**, *141*, 11929–11937. [CrossRef] [PubMed]
58. De Freitas, S.K.S.; Oliveira, F.L.; Santos, T.C.; Hisse, D.; Merlini, C.; Ronconi, C.M.; Esteves, P.M. A Carbocationic Triarylmethane-Based Porous Covalent Organic Network. *Chem. Eur. J.* **2020**, *27*, 2342–2347. [CrossRef] [PubMed]
59. Xu, H.; Gao, J.; Jiang, D. Stable, crystalline, porous, covalent organic frameworks as a platform for chiral organocatalysts. *Nat. Chem.* **2015**, *7*, 905–912. [CrossRef]
60. Liang, Y.; Xia, M.; Zhao, Y.; Wang, D.; Li, Y.; Sui, Z.; Xiao, J.; Chen, Q. Functionalized triazine-based covalent organic frameworks containing quinoline via aza-Diels-Alder reaction for enhanced lithium-sulfur batteries performance. *J. Colloid Interface Sci.* **2021**, *608*, 652–661. [CrossRef] [PubMed]
61. Lu, B.Y.; Wang, Z.Q.; Cui, F.Z.; Li, J.Y.; Han, X.H.; Qi, Q.Y.; Ma, D.L.; Jiang, G.F.; Zeng, X.X.; Zhao, X. A Covalent Organic Framework with Extended pi-Conjugated Building Units as a Highly Efficient Recipient for Lithium-Sulfur Batteries. *ACS Appl. Mater. Interfaces* **2020**, *12*, 34990–34998. [CrossRef] [PubMed]
62. Yang, C.; Jiang, K.; Zheng, Q.; Li, X.; Mao, H.; Zhong, W.; Chen, C.; Sun, B.; Zheng, H.; Zhuang, X.; et al. Chemically Stable Polyarylether-Based Metallophthalocyanine Frameworks with High Carrier Mobilities for Capacitive Energy Storage. *J. Am. Chem. Soc.* **2021**, *143*, 17701–17707. [CrossRef]
63. Wu, Y.; Yan, D.; Zhang, Z.; Matsushita, M.M.; Awaga, K. Electron Highways into Nanochannels of Covalent Organic Frameworks for High Electrical Conductivity and Energy Storage. *ACS Appl. Mater. Interfaces* **2019**, *11*, 7661–7665. [CrossRef]
64. Wang, L.; Feng, X.; Ren, L.; Piao, Q.; Zhong, J.; Wang, Y.; Li, H.; Chen, Y.; Wang, B. Flexible Solid-State Supercapacitor Based on a Metal–Organic Framework Interwoven by Electrochemically-Deposited PANI. *J. Am. Chem. Soc.* **2015**, *137*, 4920–4923. [CrossRef]
65. Srepusharawoot, P.; Scheicher, R.H.; Araújo, C.M.; Blomqvist, A.; Pinsook, U.; Ahuja, R. Ab Initio Study of Molecular Hydrogen Adsorption in Covalent Organic Framework-1. *J. Phys. Chem. C* **2009**, *113*, 8498–8504. [CrossRef]
66. Koo, B.T.; Dichtel, W.R.; Clancy, P. A classification scheme for the stacking of two-dimensional boronate ester-linked covalent organic frameworks. *J. Mater. Chem.* **2012**, *22*, 17460–17469. [CrossRef]
67. Keller, N.; Calik, M.; Sharapa, D.; Soni, H.R.; Zehetmaier, P.M.; Rager, S.; Auras, F.; Jakowetz, A.C.; Goerling, A.; Clark, T.; et al. Enforcing Extended Porphyrin J-Aggregate Stacking in Covalent Organic Frameworks. *J. Am. Chem. Soc.* **2018**, *140*, 16544–16552. [CrossRef]
68. Wang, C.; Zhao, Y.-N.; Zhu, C.-Y.; Zhang, M.; Geng, Y.; Li, Y.-G.; Su, Z.-M. A two-dimensional conductive Mo-based covalent organic framework as an efficient electrocatalyst for nitrogen fixation. *J. Mater. Chem. A* **2020**, *8*, 23599–23606. [CrossRef]
69. Lv, B.Q.; Qian, T.; Ding, H. Experimental perspective on three-dimensional topological semimetals. *Rev. Mod. Phys.* **2021**, *93*, 025002. [CrossRef]
70. Peng, H.; Huang, S.; Tranca, D.; Richard, F.; Baaziz, W.; Zhuang, X.; Samori, P.; Ciesielski, A. Quantum Capacitance through Molecular Infiltration of 7,7,8,8-Tetracyanoquinodimethane in Metal-Organic Framework/Covalent Organic Framework Hybrids. *ACS Nano* **2021**, *15*, 18580–18589. [CrossRef]
71. Xie, L.S.; Skorupskii, G.; Dincă, M. Electrically Conductive Metal–Organic Frameworks. *Chem. Rev.* **2020**, *120*, 8536–8580. [CrossRef] [PubMed]
72. Sun, L.; Campbell, M.G.; Dincă, M. Electrically Conductive Porous Metal-Organic Frameworks. *Angew. Chem. Int. Ed.* **2016**, *55*, 3566–3579. [CrossRef] [PubMed]
73. Yan, Y.; Henfling, S.; Zhang, N.N.; Krautscheid, H. Semiconductive coordination polymers with continuous pi-pi interactions and defined crystal structures. *Chem. Commun.* **2021**, *57*, 10407–10410. [CrossRef] [PubMed]
74. Li, W.-H.; Deng, W.-H.; Wang, G.-E.; Xu, G. Conductive MOFs. *EnergyChem* **2020**, *2*, 100029. [CrossRef]
75. Liu, J.; Zhou, Y.; Xie, Z.; Li, Y.; Liu, Y.; Sun, J.; Ma, Y.; Terasaki, O.; Chen, L. Conjugated Copper–Catecholate Framework Electrodes for Efficient Energy Storage. *Angew. Chem. Int. Ed.* **2019**, *59*, 1081–1086. [CrossRef] [PubMed]

76. Yang, S.; Li, X.; Qin, Y.; Cheng, Y.; Fan, W.; Lang, X.; Zheng, L.; Cao, Q. Modulating the Stacking Model of Covalent Organic Framework Isomers with Different Generation Efficiencies of Reactive Oxygen Species. *ACS Appl. Mater. Interfaces* **2021**, *13*, 29471–29481. [CrossRef] [PubMed]
77. van der Jagt, R.; Vasileiadis, A.; Veldhuizen, H.; Shao, P.; Feng, X.; Ganapathy, S.; Habisreutinger, N.C.; van der Veen, M.A.; Wang, C.; Wagemaker, M.; et al. Synthesis and Structure–Property Relationships of Polyimide Covalent Organic Frameworks for Carbon Dioxide Capture and (Aqueous) Sodium-Ion Batteries. *Chem. Mater.* **2021**, *33*, 818–833. [CrossRef] [PubMed]
78. Zhou, Z.-B.; Tian, P.-J.; Yao, J.; Lu, Y.; Qi, Q.-Y.; Zhao, X. Toward azo-linked covalent organic frameworks by developing linkage chemistry via linker exchange. *Nat. Commun.* **2022**, *13*, 2180. [CrossRef] [PubMed]
79. Zhang, Y.; Gao, Z. High performance anode material for sodium-ion batteries derived from covalent-organic frameworks. *Electrochim. Acta* **2019**, *301*, 23–28. [CrossRef]
80. Zhao, G.; Sun, Y.; Yang, Y.; Zhang, C.; An, Q.; Guo, H. Molecular engineering regulation redox-dual-active-center covalent organic frameworks-based anode for high-performance Li storage. *EcoMat* **2022**, e212221. [CrossRef]
81. Luo, X.X.; Li, W.H.; Liang, H.J.; Zhang, H.X.; Du, K.D.; Wang, X.T.; Liu, X.F.; Zhang, J.P.; Wu, X.L. Covalent Organic Framework with Highly Accessible Carbonyls and pi-Cation Effect for Advanced Potassium-Ion Batteries. *Angew. Chem.-Int. Ed.* **2022**, *61*, e202117661.
82. Xia, Z.; Jia, X.; Ge, X.; Ren, C.; Yang, Q.; Hu, J.; Chen, Z.; Han, J.; Xie, G.; Chen, S.; et al. Tailoring Electronic Structure and Size of Ultrastable Metalated Metal-Organic Frameworks with Enhanced Electroconductivity for High-Performance Super-capacitors. *Angew. Chem. Int. Ed.* **2021**, *60*, 10228–10238. [CrossRef] [PubMed]
83. Wolfson, E.R.; Schkeryantz, L.; Moscarello, E.M.; Fernandez, J.P.; Paszek, J.; Wu, Y.; Hadad, C.M.; McGrier, P.L. Al-kynyl-Based Covalent Organic Frameworks as High-Performance Anode Materials for Potassium-Ion Batteries. *ACS Appl. Mater. Interfaces* **2021**, *13*, 41628–41636. [CrossRef] [PubMed]
84. He, Y.Y.; An, N.; Meng, C.; Xie, K.-F.; Wang, X.; Dong, X.-Y.; Sun, D.; Yang, Y.; Hu, Z.-A. High-density active site COFs with a flower-like morphology for energy storage applications. *J. Mater. Chem. A* **2022**, *10*, 11030–11038. [CrossRef]
85. Ortega-Guerrero, A.; Sahabudeen, H.; Croy, A.; Dianat, A.; Dong, R.; Feng, X.; Cuniberti, G. Multiscale Modeling Strategy of 2D Covalent Organic Frameworks Confined at an Air–Water Interface. *ACS Appl. Mater. Interfaces* **2021**, *13*, 26411–26420. [CrossRef] [PubMed]
86. Han, S.; Mai, Z.; Wang, Z.; Zhang, X.; Zhu, J.; Shen, J.; Wang, J.; Wang, Y.; Zhang, Y. Covalent Organic Frame-work-Mediated Thin-Film Composite Polyamide Membranes toward Precise Ion Sieving. *ACS Appl. Mater. Interfaces* **2022**, *14*, 3427–3436. [CrossRef]
87. Zhang, C.; Wu, B.-H.; Ma, M.-Q.; Wang, Z.; Xu, Z.-K. Ultrathin metal/covalent–organic framework membranes towards ultimate separation. *Chem. Soc. Rev.* **2019**, *48*, 3811–3841. [CrossRef]
88. Guan, X.; Li, H.; Ma, Y.; Xue, M.; Fang, Q.; Yan, Y.; Valtchev, V.; Qiu, S. Chemically stable polyarylether-based covalent organic frameworks. *Nat. Chem.* **2019**, *11*, 587–594. [CrossRef]
89. Ji, X.; Kong, N.; Wang, J.; Li, W.; Xiao, Y.; Gan, S.T.; Zhang, Y.; Li, Y.; Song, X.; Xiong, Q.; et al. A Novel Top-Down Synthesis of Ultrathin 2D Boron Nanosheets for Multimodal Imaging-Guided Cancer Therapy. *Adv. Mater.* **2018**, *30*, e1803031. [CrossRef]
90. Zhou, H.G.; Xia, R.Q.; Zheng, J.; Yuan, D.; Ning, G.H.; Li, D. Acid-triggered interlayer sliding of two-dimensional cop-per(i)-organic frameworks: More metal sites for catalysis. *Chem. Sci.* **2021**, *12*, 6280–6286. [CrossRef]
91. Li, G.; Zhang, K.; Tsuru, T. Two-Dimensional Covalent Organic Framework (COF) Membranes Fabricated via the Assembly of Exfoliated COF Nanosheets. *ACS Appl. Mater. Interfaces* **2017**, *9*, 8433–8436. [CrossRef] [PubMed]
92. Burke, D.W.; Sun, C.; Castano, I.; Flanders, N.C.; Evans, A.M.; Vitaku, E.; McLeod, D.C.; Lambeth, R.H.; Chen, L.X.; Gianneschi, N.C.; et al. Acid Exfoliation of Imine-linked Covalent Organic Frameworks Enables Solution Processing into Crystalline Thin Films. *Angew. Chem. Int. Ed.* **2020**, *59*, 5165–5171. [CrossRef] [PubMed]
93. Wang, S.; Yang, Y.; Zhang, H.; Zhang, Z.; Zhang, C.; Huang, X.; Kozawa, D.; Liu, P.; Li, B.-G.; Wang, W.-J. Toward Covalent Organic Framework Metastructures. *J. Am. Chem. Soc.* **2021**, *143*, 5003–5010. [CrossRef] [PubMed]
94. Abbasi, N.M.; Xiao, Y.; Peng, L.; Duo, Y.; Wang, L.; Zhang, L.; Wang, B.; Zhang, H. Recent Advancement for the Synthesis of MXene Derivatives and Their Sensing Protocol. *Adv. Mater. Technol.* **2021**, *6*, 2001197. [CrossRef]
95. Khan, N.A.; Zhang, R.; Wu, H.; Shen, J.; Yuan, J.; Fan, C.; Cao, L.; Olson, M.A.; Jiang, Z. Solid–Vapor Interface Engineered Covalent Organic Framework Membranes for Molecular Separation. *J. Am. Chem. Soc.* **2020**, *142*, 13450–13458. [CrossRef]
96. Zhang, W.; Zhang, L.; Zhao, H.; Li, B.; Ma, H. A two-dimensional cationic covalent organic framework membrane for selective molecular sieving. *J. Mater. Chem. A* **2018**, *6*, 13331–13339. [CrossRef]
97. Li, G.; Wang, W.; Fang, Q.; Liu, F. Covalent triazine frameworks membrane with highly ordered skeleton nanopores for robust and precise molecule/ion separation. *J. Membr. Sci.* **2020**, *595*, 117525. [CrossRef]
98. Halder, A.; Kandambeth, S.; Biswal, B.P.; Kaur, G.; Roy, N.C.; Addicoat, M.; Salunke, J.K.; Banerjee, S.; Vanka, K.; Heine, T.; et al. Decoding the Morphological Diversity in Two Dimensional Crystalline Porous Polymers by Core Planarity Modulation. *Angew. Chem. Int. Ed.* **2016**, *55*, 7806–7810. [CrossRef]
99. Nguyen, V.; Grunwald, M. Microscopic Origins of Poor Crystallinity in the Synthesis of Covalent Organic Framework COF-5. *J. Am. Chem. Soc.* **2018**, *140*, 3306–3311. [CrossRef]
100. Koo, B.T.; Heden, R.F.; Clancy, P. Nucleation and growth of 2D covalent organic frameworks: Polymerization and crystallization of COF monomers. *Phys. Chem. Chem. Phys.* **2017**, *19*, 9745–9754. [CrossRef] [PubMed]

101. Halder, A.; Karak, S.; Addicoat, M.; Bera, S.; Chakraborty, A.; Kunjattu, S.H.; Pachfule, P.; Heine, T.; Banerjee, R. Ultrastable Imine-Based Covalent Organic Frameworks for Sulfuric Acid Recovery: An Effect of Interlayer Hydrogen Bonding. *Angew. Chem. Int. Ed.* **2018**, *57*, 5797–5802. [CrossRef] [PubMed]
102. Kandambeth, S.; Biswal, B.P.; Chaudhari, H.D.; Rout, K.C.; Kunjattu H, S.; Mitra, S.; Karak, S.; Das, A.; Mukherjee, R.; Kharul, U.K.; et al. Selective Molecular Sieving in Self-Standing Porous Covalent-Organic-Framework Membranes. *Adv. Mater.* **2016**, *29*, 1603945. [CrossRef] [PubMed]
103. Fan, H.; Gu, J.; Meng, H.; Knebel, A.; Caro, J. High-Flux Membranes Based on the Covalent Organic Framework COF-LZU1 for Selective Dye Separation by Nanofiltration. *Angew. Chem. Int. Ed.* **2018**, *57*, 4083–4087. [CrossRef]
104. Zhang, H.; Gu, C.; Yao, M.-S.; Kitagawa, S. Hybridization of Emerging Crystalline Porous Materials: Synthesis Dimensionality and Electrochemical Energy Storage Application. *Adv. Energy Mater.* **2022**, *12*, 2100321. [CrossRef]
105. Xu, Z.; Deng, W.; Wang, X. 3D Hierarchical Carbon-Rich Micro-/Nanomaterials for Energy Storage and Catalysis. *Electrochem. Energy Rev.* **2021**, *4*, 269–335. [CrossRef]
106. Hu, Y.; Wayment, L.J.; Haslam, C.; Yang, X.; Lee, S.-H.; Jin, Y.; Zhang, W. Covalent organic framework based lithium-ion battery: Fundamental, design and characterization. *EnergyChem* **2021**, *3*, 100048. [CrossRef]
107. Zhao, G.; Zhang, Y.; Gao, Z.; Li, H.; Liu, S.; Cai, S.; Yang, X.; Guo, H.; Sun, X. Dual Active Site of the Azo and Carbon-yl-Modified Covalent Organic Framework for High-Performance Li Storage. *ACS Energy Lett.* **2020**, *5*, 1022–1031. [CrossRef]
108. Zheng, Y.; Yao, Y.; Ou, J.; Li, M.; Luo, D.; Dou, H.; Li, Z.; Amine, K.; Yu, A.; Chen, Z. A review of composite solid-state electrolytes for lithium batteries: Fundamentals, key materials and advanced structures. *Chem. Soc. Rev.* **2020**, *49*, 8790–8839. [CrossRef]
109. Huang, N.; Wang, P.; Jiang, D. Covalent organic frameworks: A materials platform for structural and functional designs. *Nat. Rev. Mater.* **2016**, *1*, 16068. [CrossRef]
110. Hao, Z.; Zhao, Q.; Tang, J.; Zhang, Q.; Liu, J.; Jin, Y.; Wang, H. Functional separators towards the suppression of lithium dendrites for rechargeable high-energy batteries. *Mater. Horizons* **2020**, *8*, 12–32. [CrossRef] [PubMed]
111. Shi, R.; Liu, L.; Lu, Y.; Wang, C.; Li, Y.; Li, L.; Yan, Z.; Chen, J. Nitrogen-rich covalent organic frameworks with multiple carbonyls for high-performance sodium batteries. *Nat. Commun.* **2020**, *11*, 178. [CrossRef]
112. Huang, J.; Golomb, M.J.; Kavanagh, S.R.; Tolborg, K.; Ganose, A.M.; Walsh, A. Band gap opening from displacive instabilities in layered covalent-organic frameworks. *J. Mater. Chem. A* **2022**, *10*, 13500–13507. [CrossRef]
113. Zhai, L.; Wei, W.; Ma, B.; Ye, W.; Wang, J.; Chen, W.; Yang, X.; Cui, S.; Wu, Z.; Soutis, C.; et al. Cationic Covalent Organic Frameworks for Fabricating an Efficient Triboelectric Nanogenerator. *ACS Mater. Lett.* **2020**, *2*, 1691–1697. [CrossRef]
114. Kong, L.; Liu, M.; Huang, H.; Xu, Y.; Bu, X.-H. Metal/Covalent-Organic Framework Based Cathodes for Metal-Ion Batteries. *Adv. Energy Mater.* **2022**, *12*, 2100172. [CrossRef]
115. Liu, M.; Kong, L.; Wang, X.; He, J.; Bu, X. Engineering Bimetal Synergistic Electrocatalysts Based on Metal–Organic Frameworks for Efficient Oxygen Evolution. *Small* **2019**, *15*, e1903410. [CrossRef]
116. Yang, J.; Bin Tu, B.; Zhang, G.; Liu, P.; Hu, K.; Wang, J.; Yan, Z.; Huang, Z.; Fang, M.; Hou, J.; et al. Advancing osmotic power generation by covalent organic framework monolayer. *Nat. Nanotechnol.* **2022**, *17*, 622–628. [CrossRef]
117. Xu, F.; Yang, S.; Chen, X.; Liu, Q.; Li, H.; Wang, H.; Wei, B.; Jiang, D. Energy-storage covalent organic frameworks: Improving performance via engineering polysulfide chains on walls. *Chem. Sci.* **2019**, *10*, 6001–6006. [CrossRef]
118. Meng, Y.; Luo, Y.; Shi, J.; Ding, H.; Lang, X.; Chen, W.; Zheng, A.; Sun, J.; Wang, C. 2D and 3D Porphyrinic Covalent Organic Frameworks: The Influence of Dimensionality on Functionality. *Angew. Chem. Int. Ed.* **2019**, *59*, 3624–3629. [CrossRef]
119. Ma, Y.-X.; Li, Z.-J.; Wei, L.; Ding, S.-Y.; Zhang, Y.-B.; Wang, W. A Dynamic Three-Dimensional Covalent Organic Framework. *J. Am. Chem. Soc.* **2017**, *139*, 4995–4998. [CrossRef]
120. Fang, Q.; Sui, C.; Wang, C.; Zhai, T.; Zhang, J.; Liang, J.; Guo, H.; Sandoz-Rosado, E.; Lou, J. Strong and flaw-insensitive two-dimensional covalent organic frameworks. *Matter* **2021**, *4*, 1017–1028. [CrossRef]
121. Liu, X.; Li, J.; Gui, B.; Lin, G.; Fu, Q.; Yin, S.; Liu, X.; Sun, J.; Wang, C. A Crystalline Three-Dimensional Covalent Organic Framework with Flexible Building Blocks. *J. Am. Chem. Soc.* **2021**, *143*, 2123–2129. [CrossRef]
122. Li, T.; Zhang, W.-D.; Liu, Y.; Li, Y.; Cheng, C.; Zhu, H.; Yan, X.; Li, Z.; Gu, Z.-G. A two-dimensional semiconducting covalent organic framework with nickel(ii) coordination for high capacitive performance. *J. Mater. Chem. A* **2019**, *7*, 19676–19681. [CrossRef]
123. Colson, J.W.; Woll, A.R.; Mukherjee, A.; Levendorf, M.P.; Spitler, E.L.; Shields, V.B.; Spencer, M.G.; Park, J.; Dichtel, W.R. Oriented 2D Covalent Organic Framework Thin Films on Single-Layer Graphene. *Science* **2011**, *332*, 228–231. [CrossRef]
124. Ding, S.-Y.; Wang, W. Covalent organic frameworks (COFs): From design to applications. *Chem. Soc. Rev.* **2012**, *42*, 548–568. [CrossRef]
125. Spitler, E.L.; Koo, B.T.; Novotney, J.L.; Colson, J.W.; Uribe-Romo, F.J.; Gutierrez, G.D.; Clancy, P.; Dichtel, W.R. A 2D Covalent Organic Framework with 4.7-nm Pores and Insight into Its Interlayer Stacking. *J. Am. Chem. Soc.* **2011**, *133*, 19416–19421. [CrossRef]
126. Yan, W.; Gao, X.; Yang, J.; Xiong, X.; Xia, S.; Huang, W.; Chen, Y.; Fu, L.; Zhu, Y.; Wu, Y. Boosting Polysulfide Catalytic Conversion and Facilitating Li^+ Transportation by Ion-Selective COFs Composite Nanowire for Li-S Batteries. *Small* **2022**, *18*, 2106679. [CrossRef]
127. Dai, Y.; Wang, Y.; Li, X.; Cui, M.; Gao, Y.; Xu, H.; Xu, X. In situ form core-shell carbon nanotube-imide COF composite for high performance negative electrode of pseudocapacitor. *Electrochim. Acta* **2022**, *421*. [CrossRef]

128. Geng, Q.; Wang, H.; Wang, J.; Hong, J.; Sun, W.; Wu, Y.; Wang, Y. Boosting the Capacity of Aqueous Li-Ion Capacitors via Pinpoint Surgery in Nanocoral-Like Covalent Organic Frameworks. *Small Methods* **2022**. [CrossRef]
129. Haldar, S.; Rase, D.; Shekhar, P.; Jain, C.; Vinod, C.P.; Zhang, E.; Shupletsov, L.; Kaskel, S.; Vaidhyanathan, R. Incorporating Conducting Polypyrrole into a Polyimide COF for Carbon-Free Ultra-High Energy Supercapacitor. *Adv. Energy Mater.* **2022**, *12*. [CrossRef]
130. Kang, K.; Wu, Z.; Zhao, M.; Li, Z.; Ma, Y.; Zhang, J.; Wang, Y.; Sajjad, M.; Tao, R.; Qiu, L. A nanostructured covalent organic framework with readily accessible triphenylstibine moieties for high-performance supercapacitors. *Chem. Commun.* **2022**, *58*, 3649–3652. [CrossRef] [PubMed]
131. Yan, W.; Yu, F.; Jiang, Y.; Su, J.; Ke, S.-W.; Tie, Z.; Zuo, J.-L.; Jin, Z. Self-Assembly Construction of Carbon Nanotube Network-Threaded Tetrathiafulvalene-Bridging Covalent Organic Framework Composite Anodes for High-Performance Hybrid Lithium-Ion Capacitors. *Small Struct.* **2022**. [CrossRef]
132. Zhang, Y.; Wu, Y.; An, Y.; Wei, C.; Tan, L.; Xi, B.; Xiong, S.; Feng, J. Ultrastable and High-Rate 2D Siloxene Anode Enabled by Covalent Organic Framework Engineering for Advanced Lithium-lon Batteries. *Small Methods* **2022**, *6*, 2200306. [CrossRef] [PubMed]
133. Yang, Z.; Liu, J.; Li, Y.; Zhang, G.; Xing, G.; Chen, L. Arylamine-Linked 2D Covalent Organic Frameworks for Efficient Pseudocapacitive Energy Storage. *Angew. Chem. Int. Ed.* **2021**, *60*, 20754–20759. [CrossRef] [PubMed]
134. Singh, V.; Kim, J.; Kang, B.; Moon, J.; Kim, S.; Kim, W.Y.; Byon, H.R. Thiazole-Linked Covalent Organic Framework Promoting Fast Two-Electron Transfer for Lithium-Organic Batteries. *Adv. Energy Mater.* **2021**, *11*, 2003735. [CrossRef]
135. Yusran, Y.; Li, H.; Guan, X.; Li, D.; Tang, L.; Xue, M.; Zhuang, Z.; Yan, Y.; Valtchev, V.; Qiu, S.; et al. Exfoliated Mesoporous 2D Covalent Organic Frameworks for High-Rate Electrochemical Double-Layer Capacitors. *Adv. Mater.* **2020**, *32*, 1907289. [CrossRef]
136. An, N.; Guo, Z.; Xin, J.; He, Y.; Xie, K.; Sun, D.; Dong, X.; Hu, Z. Hierarchical porous covalent organic framework/graphene aerogel electrode for high-performance supercapacitors. *J. Mater. Chem. A* **2021**, *9*, 16824–16833. [CrossRef]
137. Amin, K.; Zhang, J.; Zhou, H.-Y.; Lu, R.; Zhang, M.; Ashraf, N.; YueLi, C.; Mao, L.; Faul, C.F.J.; Wei, Z. Surface controlled pseudo-capacitive reactions enabling ultra-fast charging and long-life organic lithium ion batteries. *Sustain. Energy Fuels* **2020**, *4*, 4179–4185. [CrossRef]
138. Kong, X.; Zhou, S.; Strømme, M.; Xu, C. Redox active covalent organic framework-based conductive nanofibers for flexible energy storage device. *Carbon* **2021**, *171*, 248–256. [CrossRef]
139. Liu, S.; Yao, L.; Lu, Y.; Hua, X.; Liu, J.; Yang, Z.; Wei, H.; Mai, Y. All-organic covalent organic framework/polyaniline composites as stable electrode for high-performance supercapacitors. *Mater. Lett.* **2018**, *236*, 354–357. [CrossRef]